

Supporting Information

for

Self-Assembly of Rigid Amphiphilic Graft Cyclic-brush Copolymers to Nanochannels Using Dissipative Particle Dynamics Simulation

Meng Du^{a#} Xinrong Yan^{a#}, Nanrong Zhao^a Xin Wang^a and Dingguo Xu^{a,b,*}

^a *MOE Key Laboratory of Green Chemistry and Technology, College of Chemistry,
Sichuan University, Chengdu, Sichuan 610064, PR China*

^b *Research Center for Materials Genome Engineering, Sichuan University, Chengdu,
Sichuan 610065, PR China*

Both authors contributed equally.

* To whom correspondence should be addressed: E-mail: dgxu@scu.edu.cn (D.X.) Tel:

86-28-85406156

Contents

Figure S1: Snapshots of the last frame with the parameters set to $a_{AS}=25$, $a_{BS}=65$ and $a_{AB}=45$, which indicates hydrophilic beads are inside and hydrophobic beads are outside.

Figure S2-S36: Snapshots of the last frames for all 605 models with different interaction parameters and settings of copolymer sizes and concentrations.

Figure S37. Summary of the phase transformation along the changes of simulation parameters, in which the interaction affinity of A and S decreases and the interaction between A and B increases. Herein, the parameters of $\varphi=40$ and $N=20$.

Figure S38. Summary of the phase transformation along the changes of simulation parameters, in which the repulsion of B and S beads increases. Herein, the parameters of $\varphi=40$ and $N=20$. Meanwhile, there is a big interaction parameter for A and B beads.

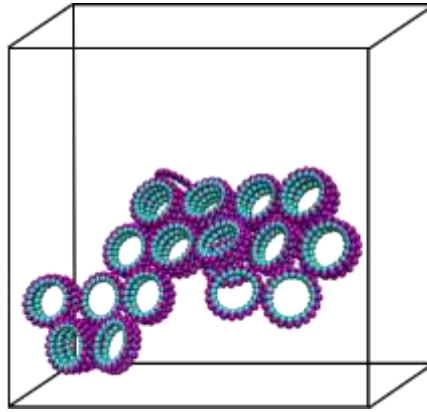


Figure S1. The snapshot of last frame extracted from MD trajectory in $\varphi=40$, $N=20$, $a_{AS}=25$, $a_{BS}=65$ and $a_{AB}=45$, which indicates hydrophilic beads are inside and hydrophobic beads are outside.

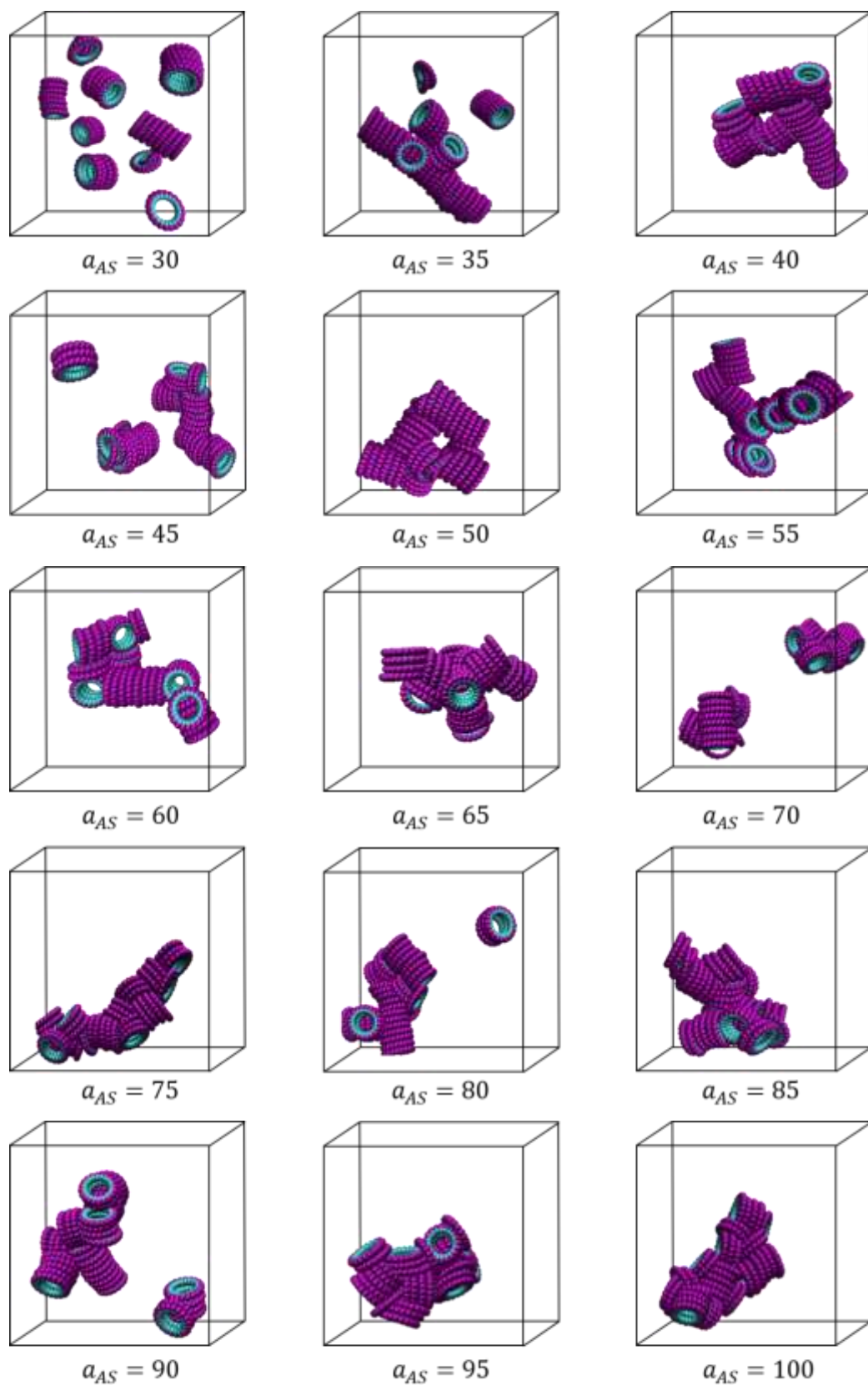


Figure S2. The snapshots of last frames extracted from MD trajectories in different values of a_{AS} , in which $\varphi=40$, $N=20$, $a_{BS}=25$ and $a_{AB}=25$.

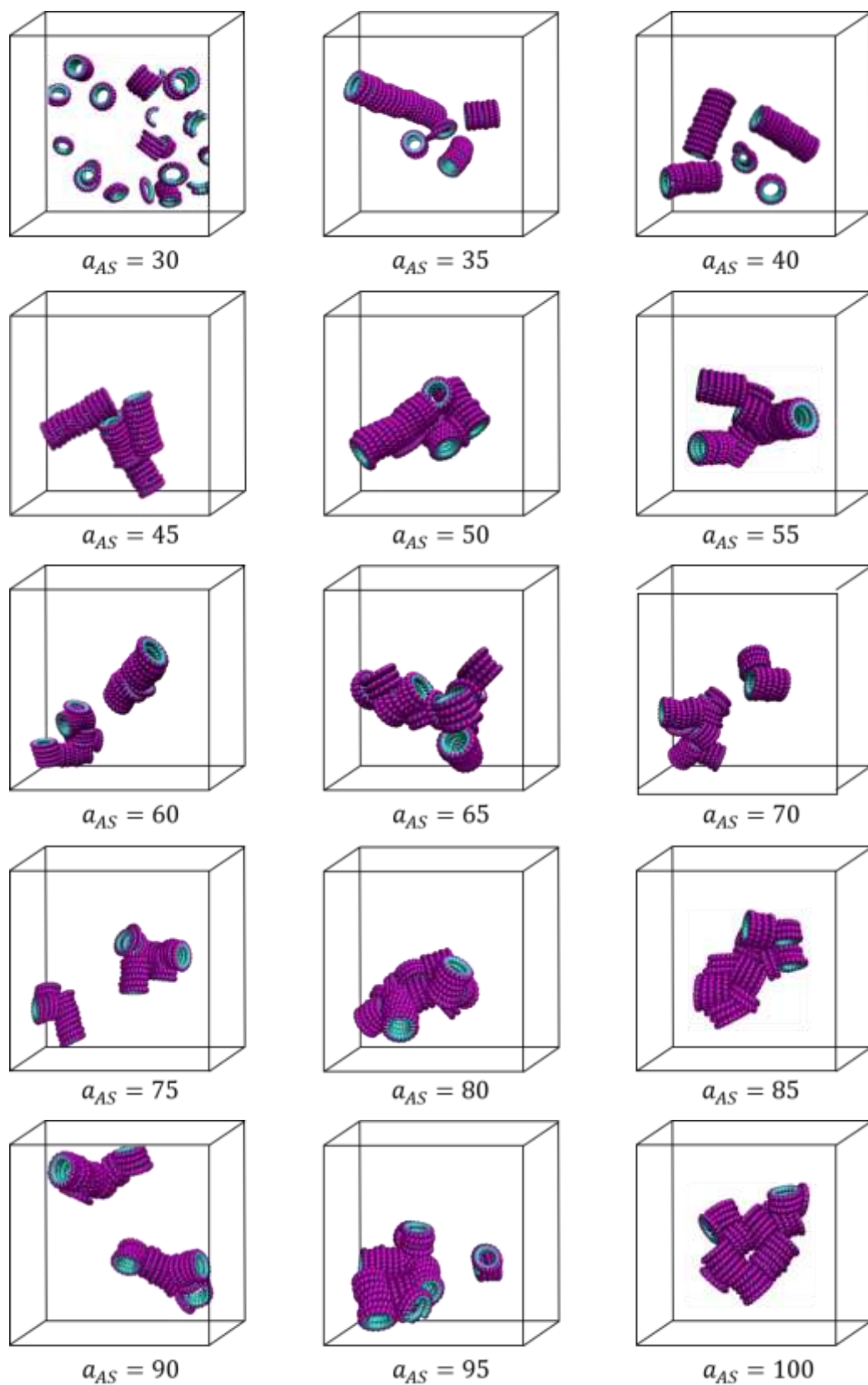


Figure S3. The snapshots of last frames extracted from MD trajectories in different values of a_{AS} , in which $\varphi=40$, $N=20$, $a_{BS}=25$ and $a_{AB}=30$.

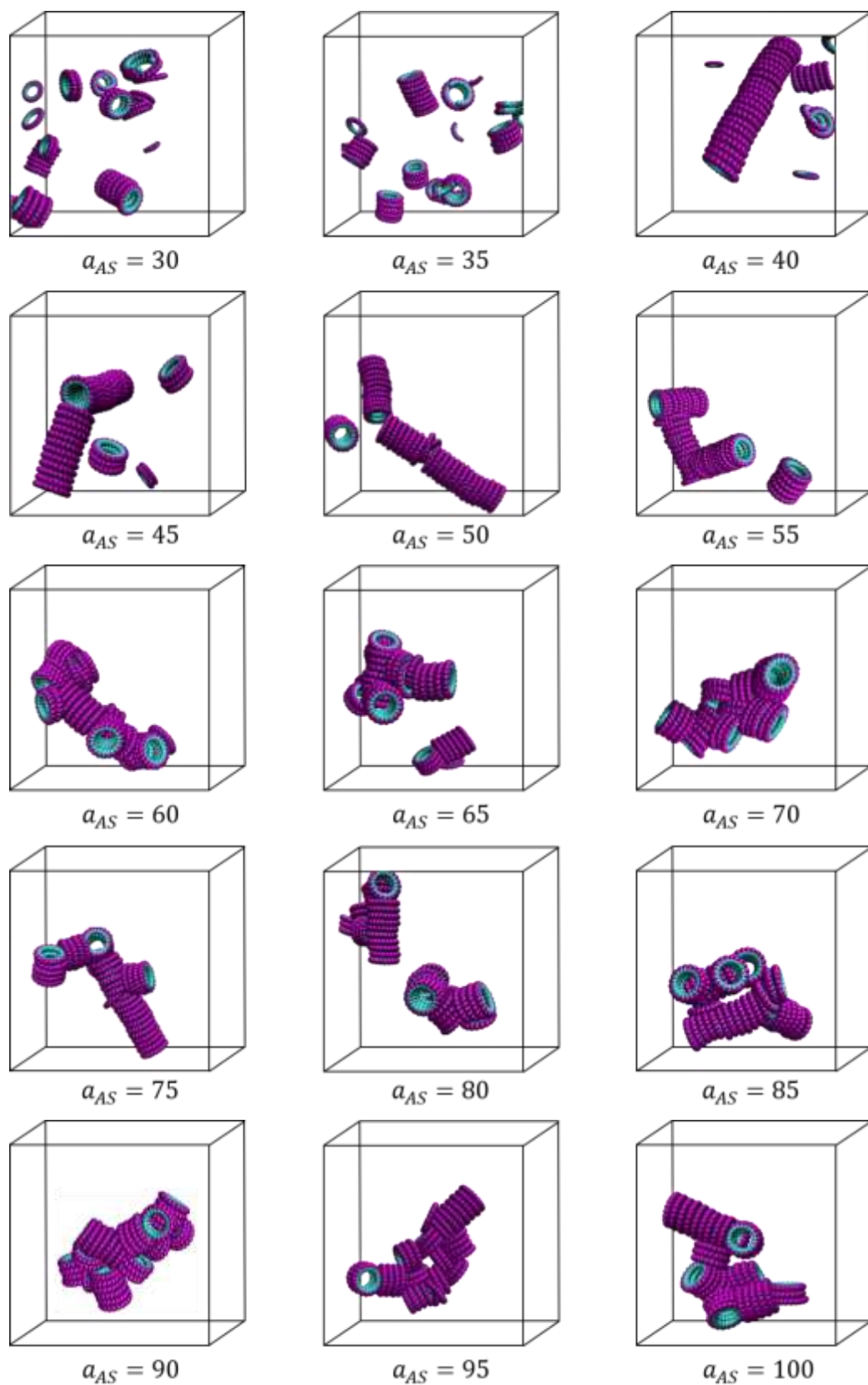


Figure S4. The snapshots of last frames extracted from MD trajectories in different values of a_{AS} , in which $\varphi=40$, $N=20$, $a_{BS}=25$ and $a_{AB}=35$.

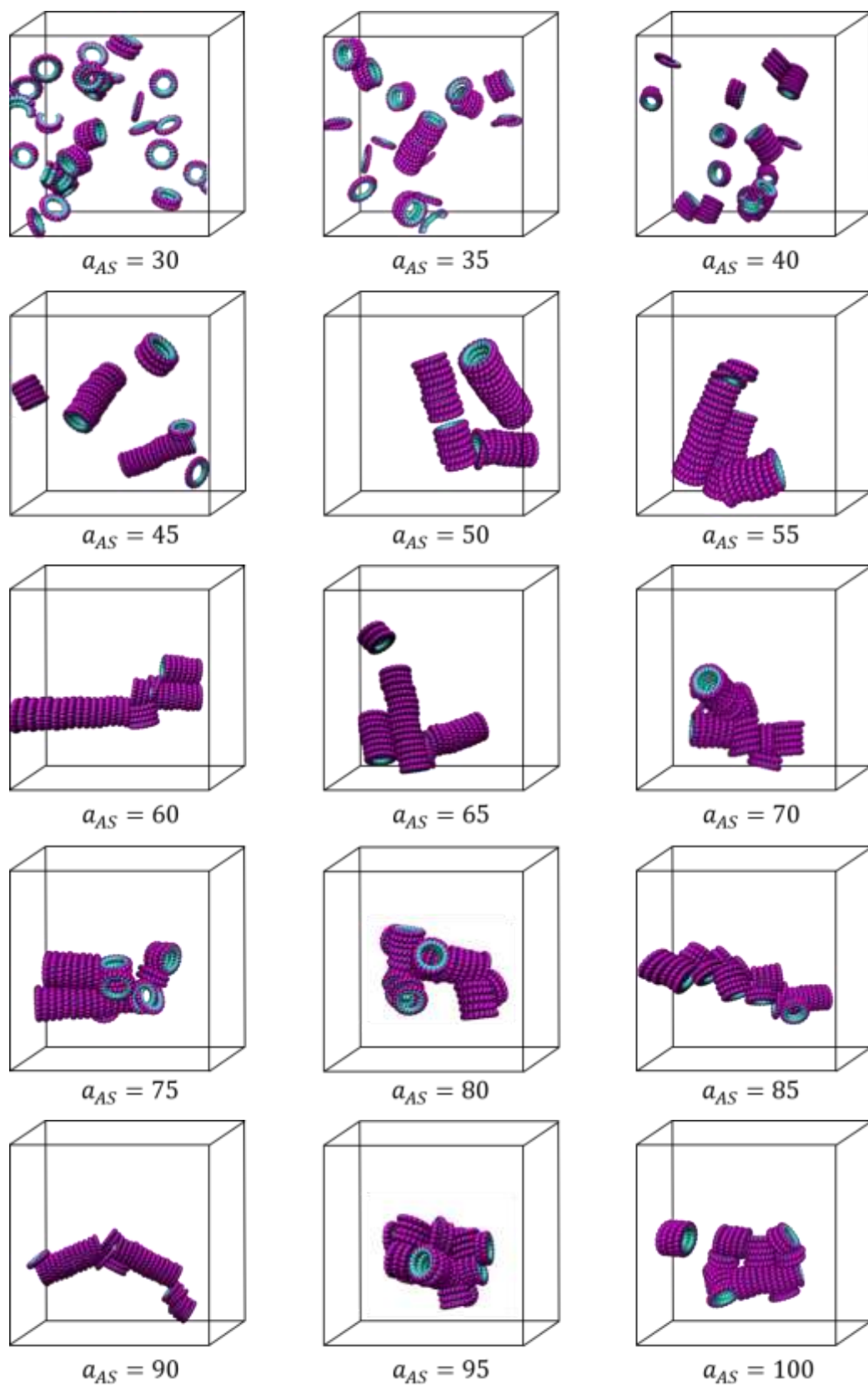


Figure S5. The snapshots of last frames extracted from MD trajectories in different values of a_{AS} , in which $\varphi=40$, $N=20$, $a_{BS}=25$ and $a_{AB}=40$.

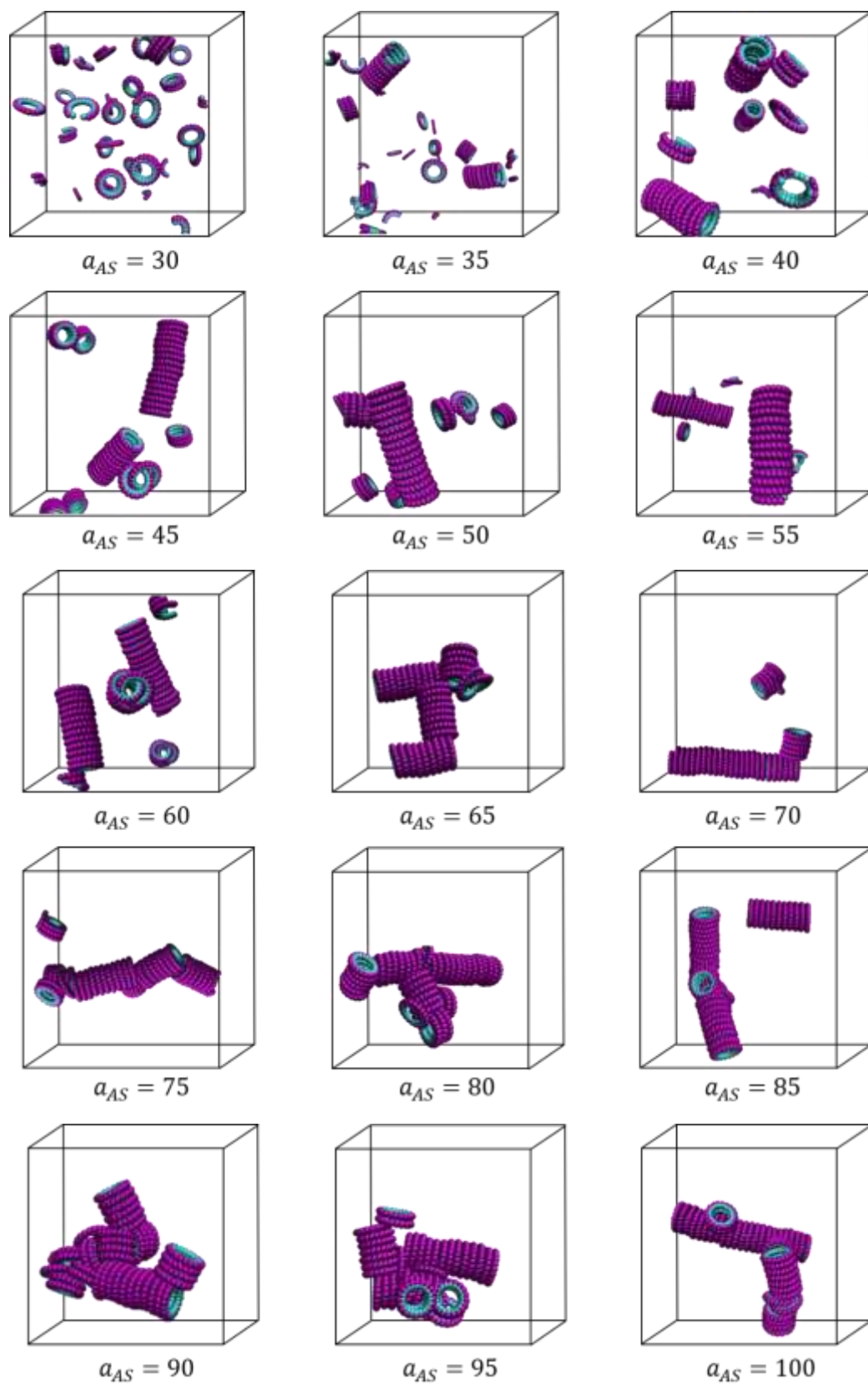


Figure S6. The snapshots of last frames extracted from MD trajectories in different values of a_{AS} , in which $\varphi=40$, $N=20$, $a_{BS}=25$ and $a_{AB}=45$.

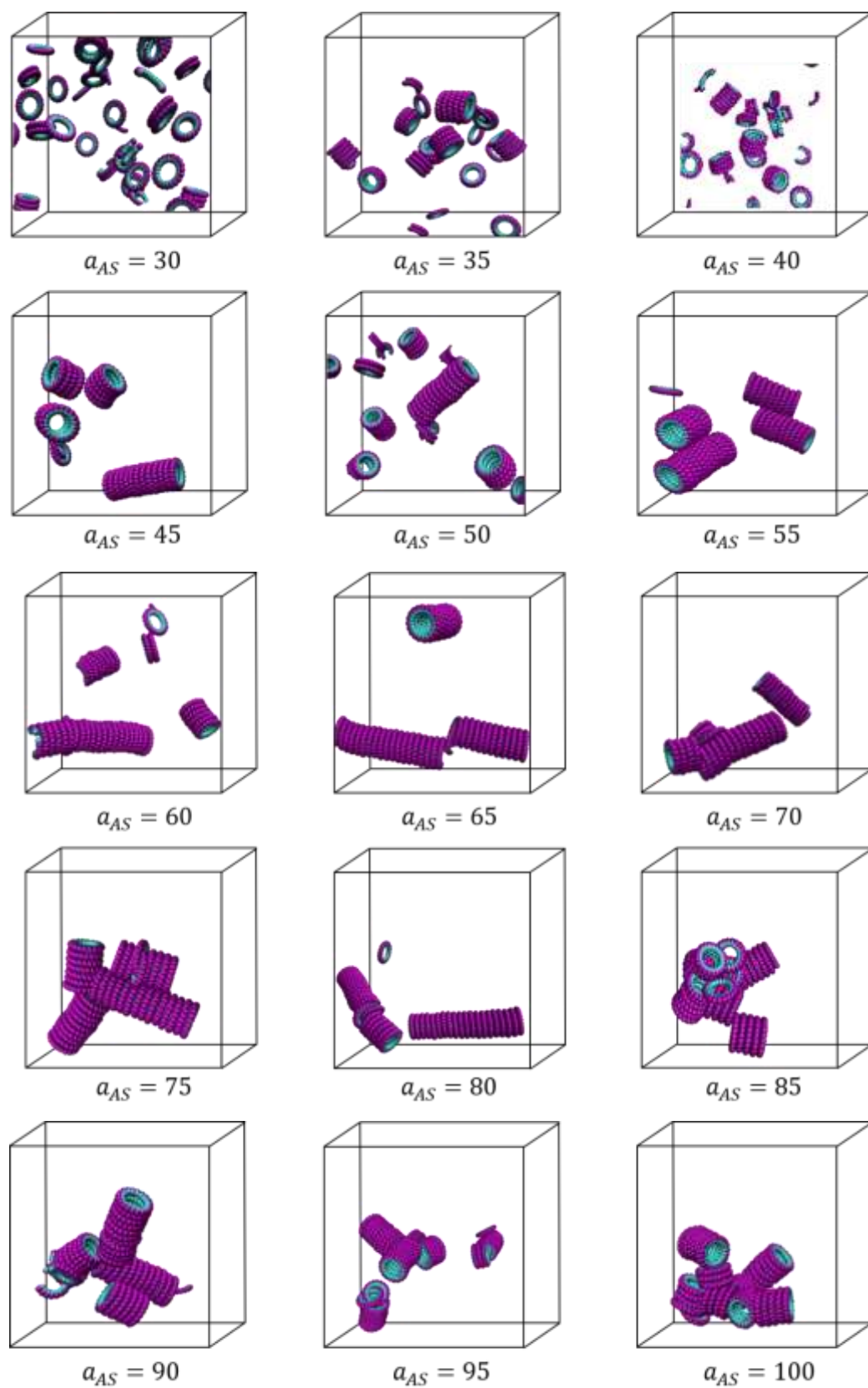


Figure S7. The snapshots of last frames extracted from MD trajectories in different values of a_{AS} , in which $\varphi=40$, $N=20$, $a_{BS}=25$ and $a_{AB}=50$.

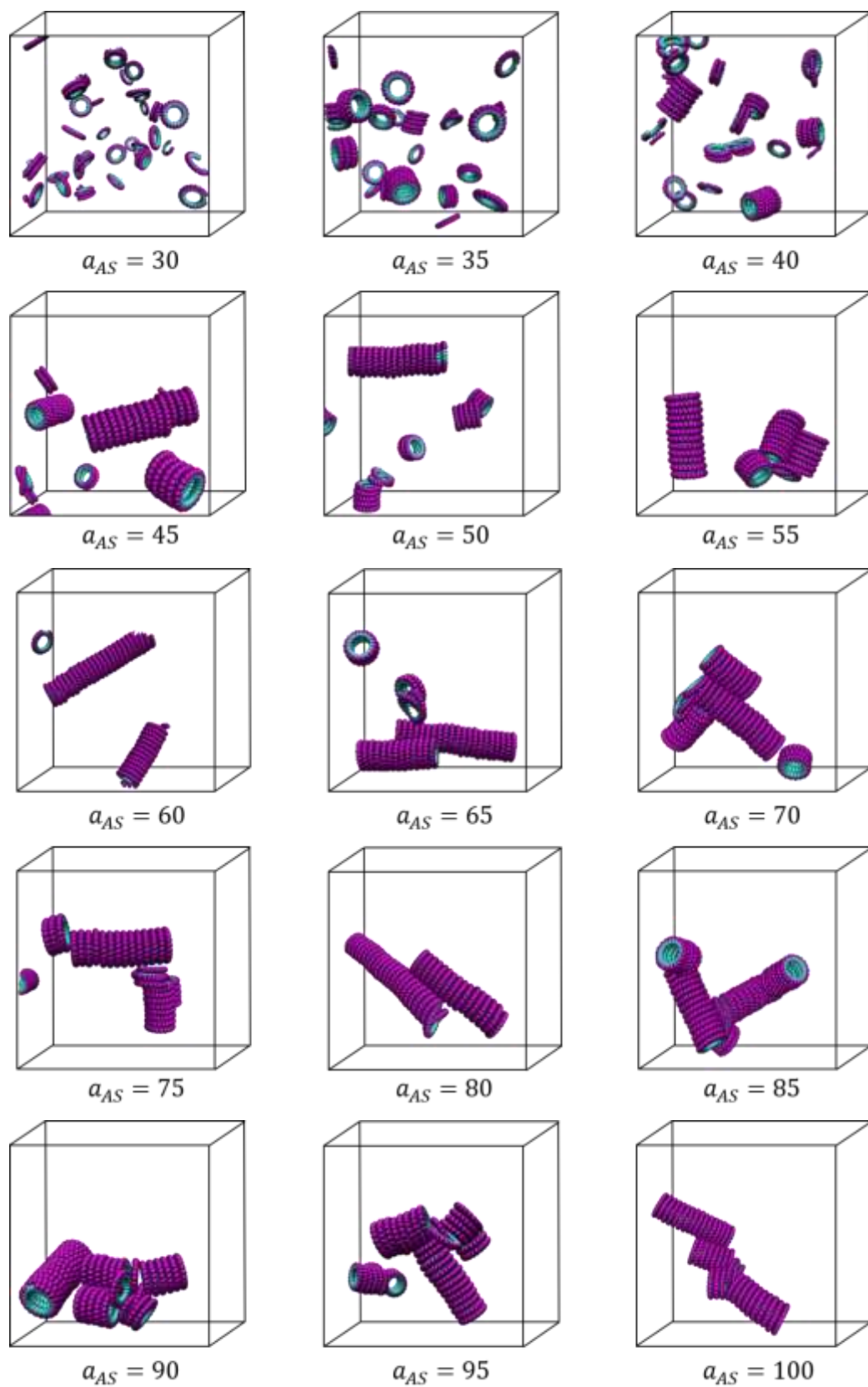


Figure S8. The snapshots of last frames extracted from MD trajectories in different values of a_{AS} , in which $\varphi=40$, $N=20$, $a_{BS}=25$ and $a_{AB}=55$.

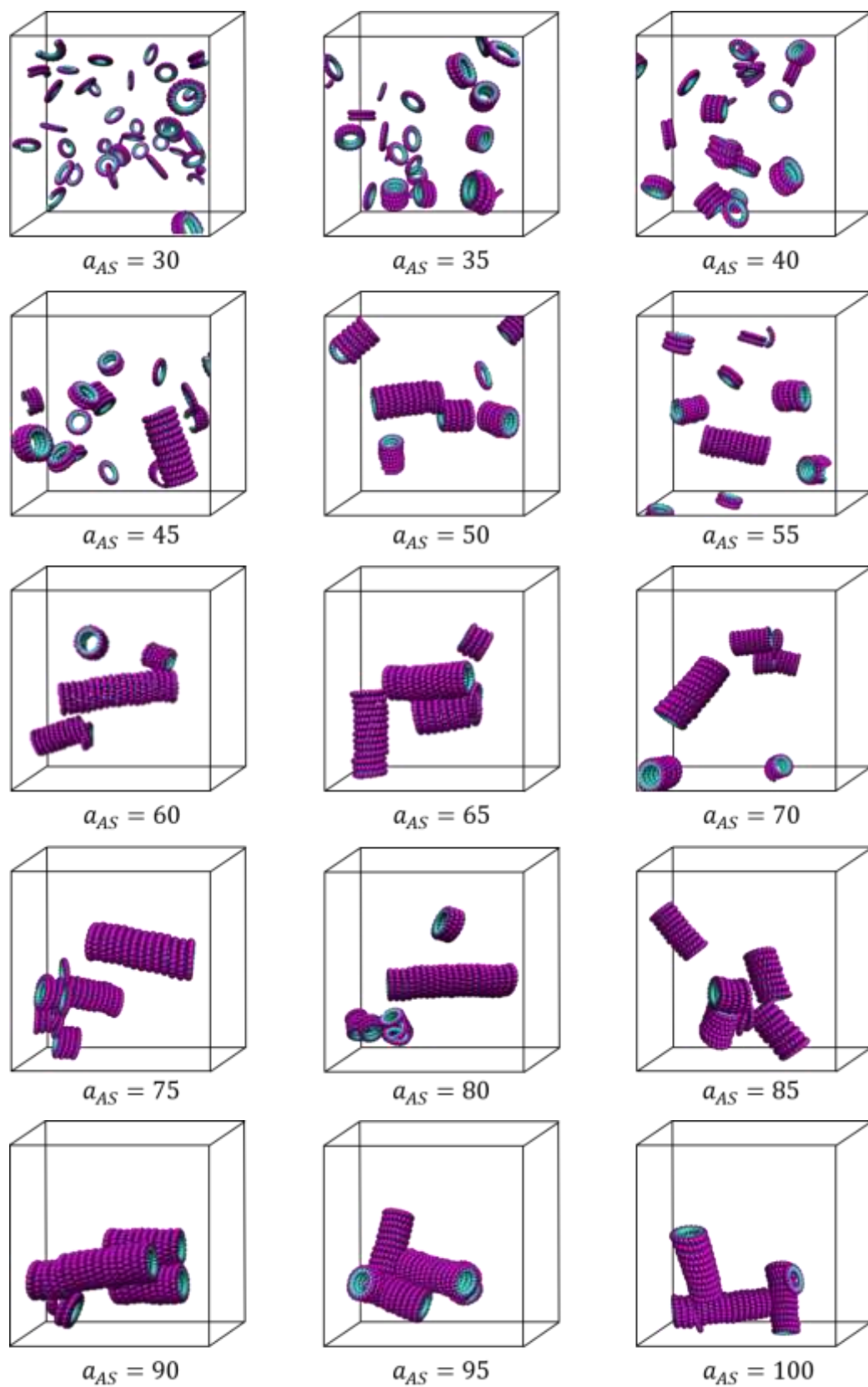


Figure S9. The snapshots of last frames extracted from MD trajectories in different values of a_{AS} , in which $\varphi=40$, $N=20$, $a_{BS}=25$ and $a_{AB}=60$.

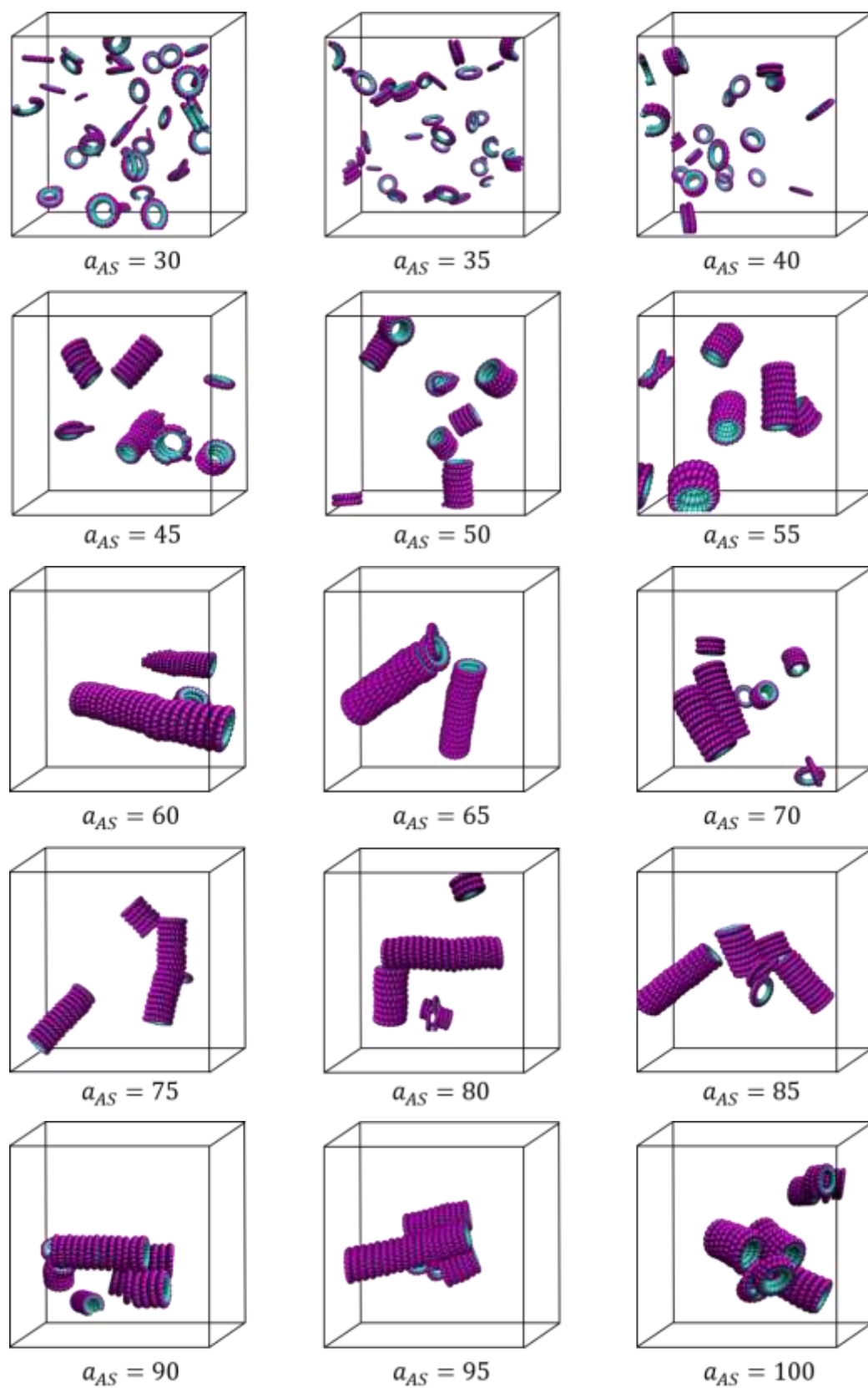


Figure S10. The snapshots of last frames extracted from MD trajectories in different values of a_{AS} , in which $\varphi=40$, $N=20$, $a_{BS}=25$ and $a_{AB}=65$.

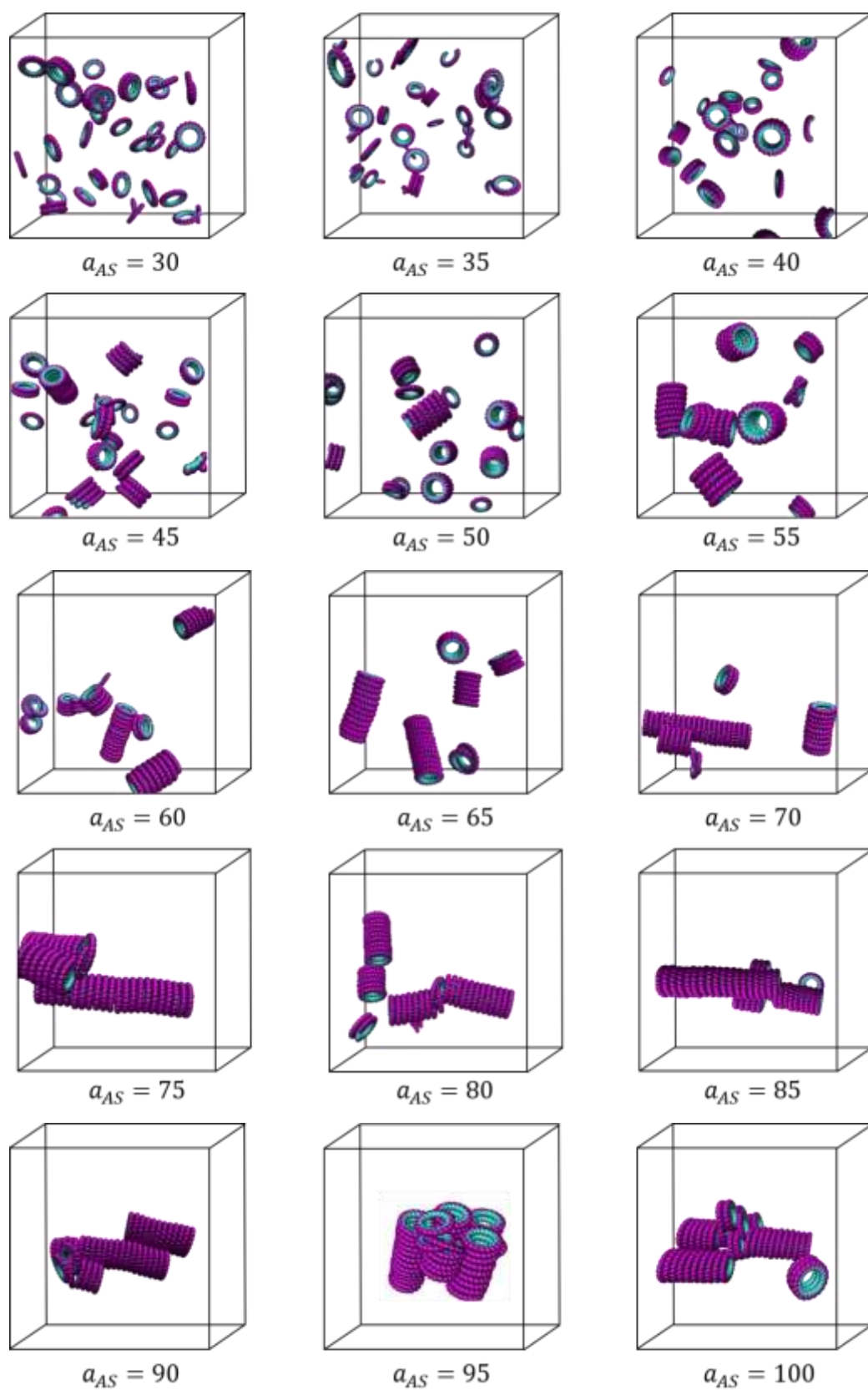


Figure S11. The snapshots of last frames extracted from MD trajectories in different values of a_{AS} , in which $\varphi=40$, $N=20$, $a_{BS}=25$ and $a_{AB}=70$.

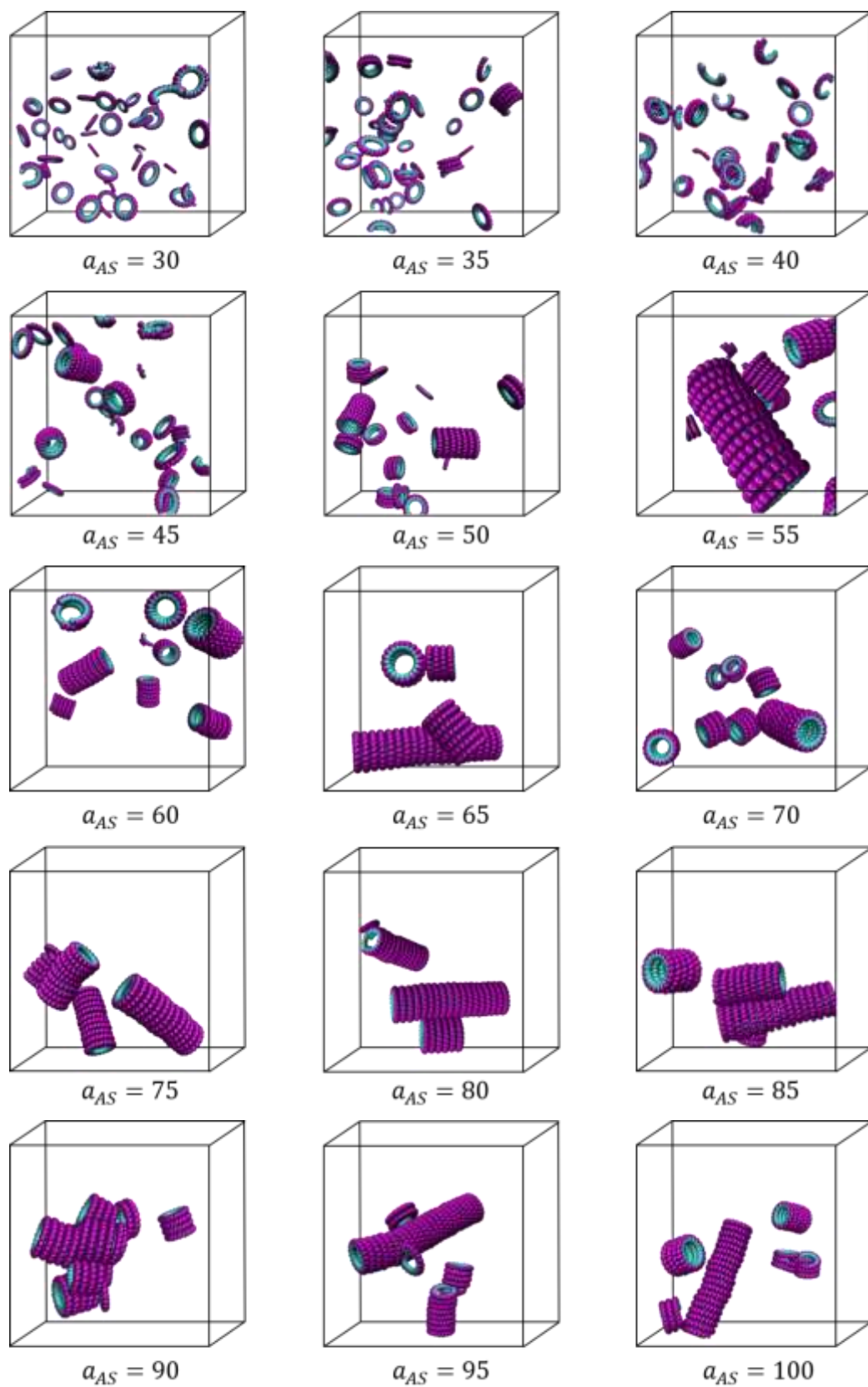


Figure S12. The snapshots of last frames extracted from MD trajectories in different values of a_{AS} , in which $\varphi=40$, $N=20$, $a_{BS}=25$ and $a_{AB}=75$.

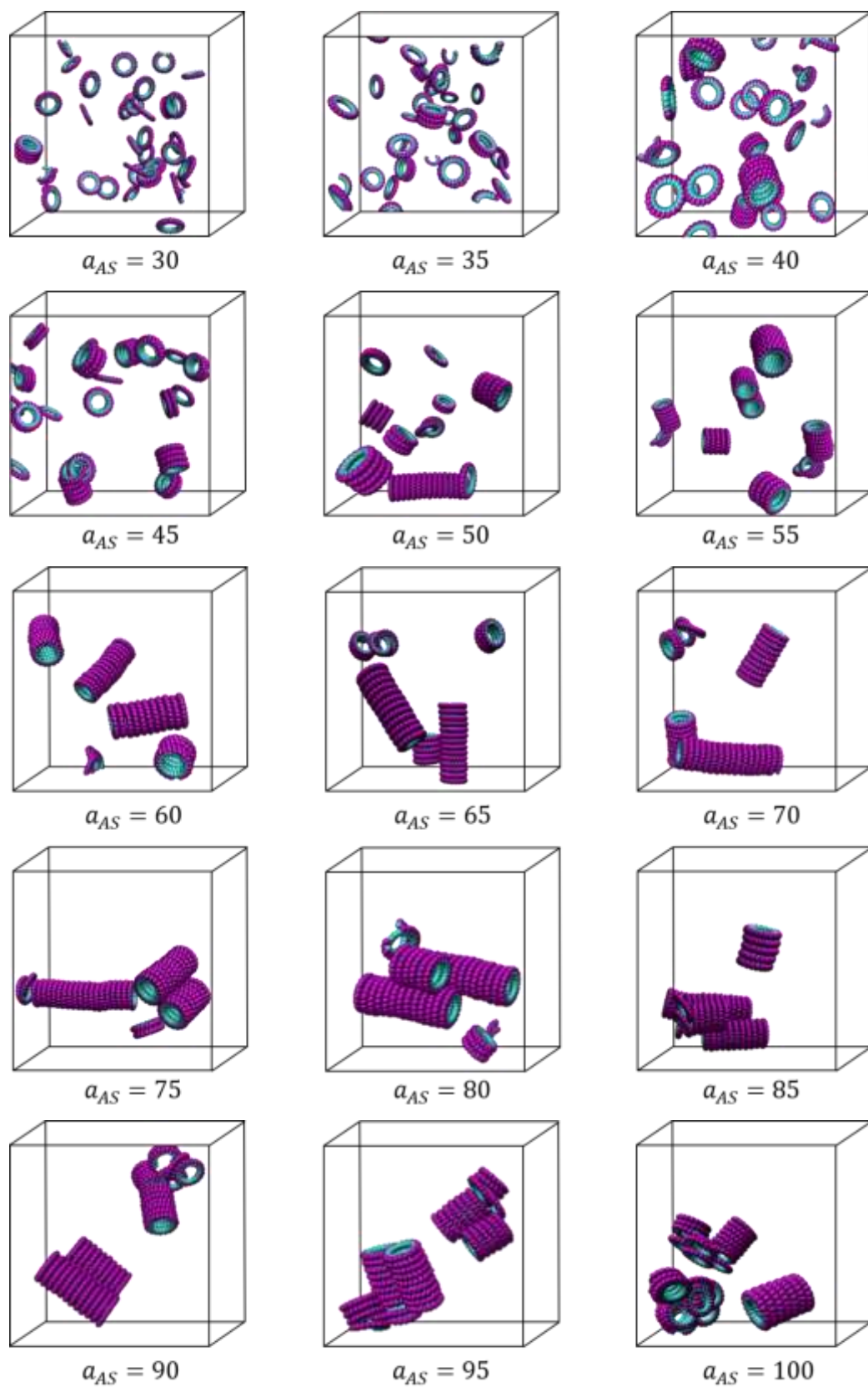


Figure S13. The snapshots of last frames extracted from MD trajectories in different values of a_{AS} , in which $\varphi=40$, $N=20$, $a_{BS}=25$ and $a_{AB}=80$.

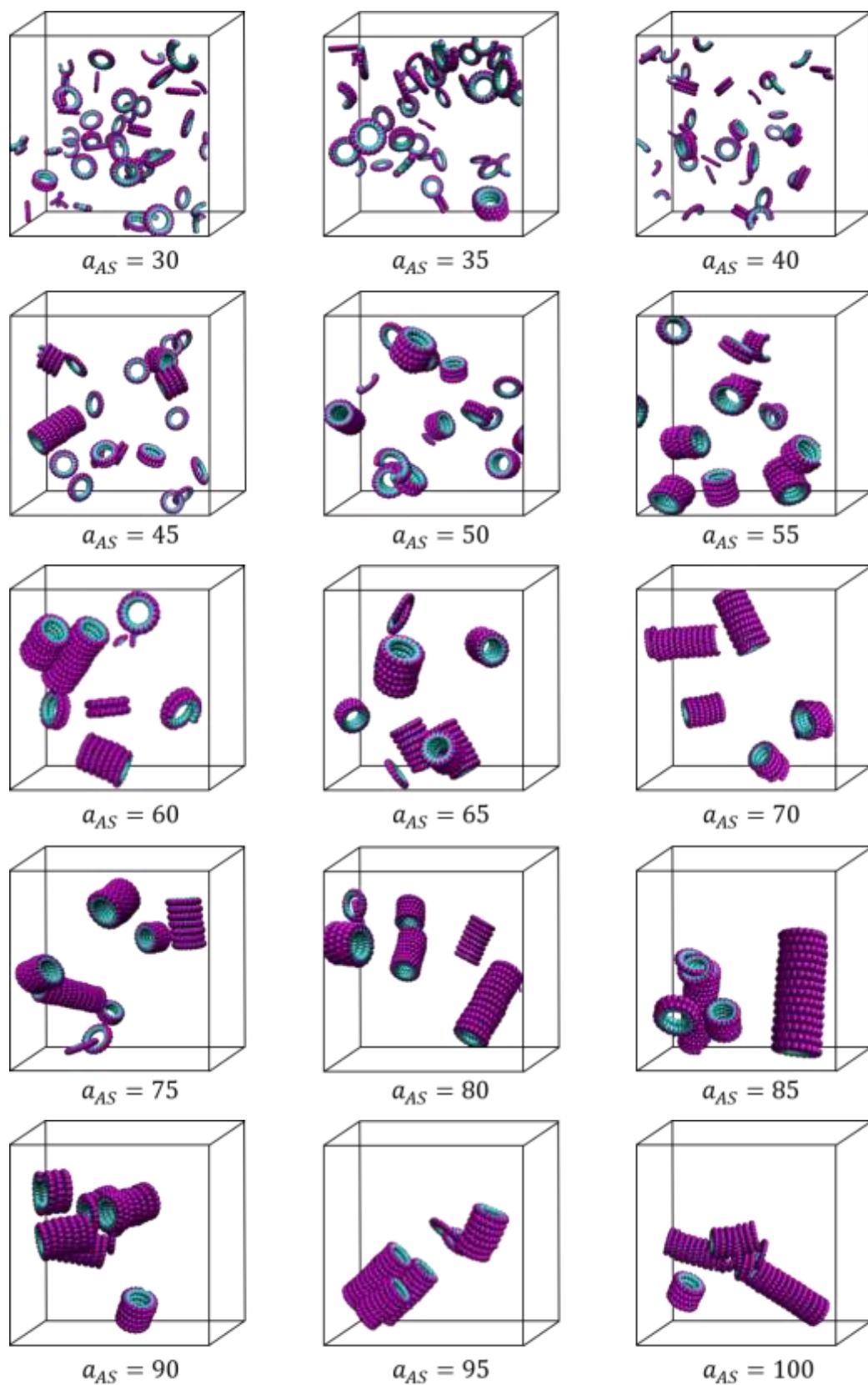


Figure S14. The snapshots of last frames extracted from MD trajectories in different values of a_{AS} , in which $\varphi=40$, $N=20$, $a_{BS}=25$ and $a_{AB}=85$.

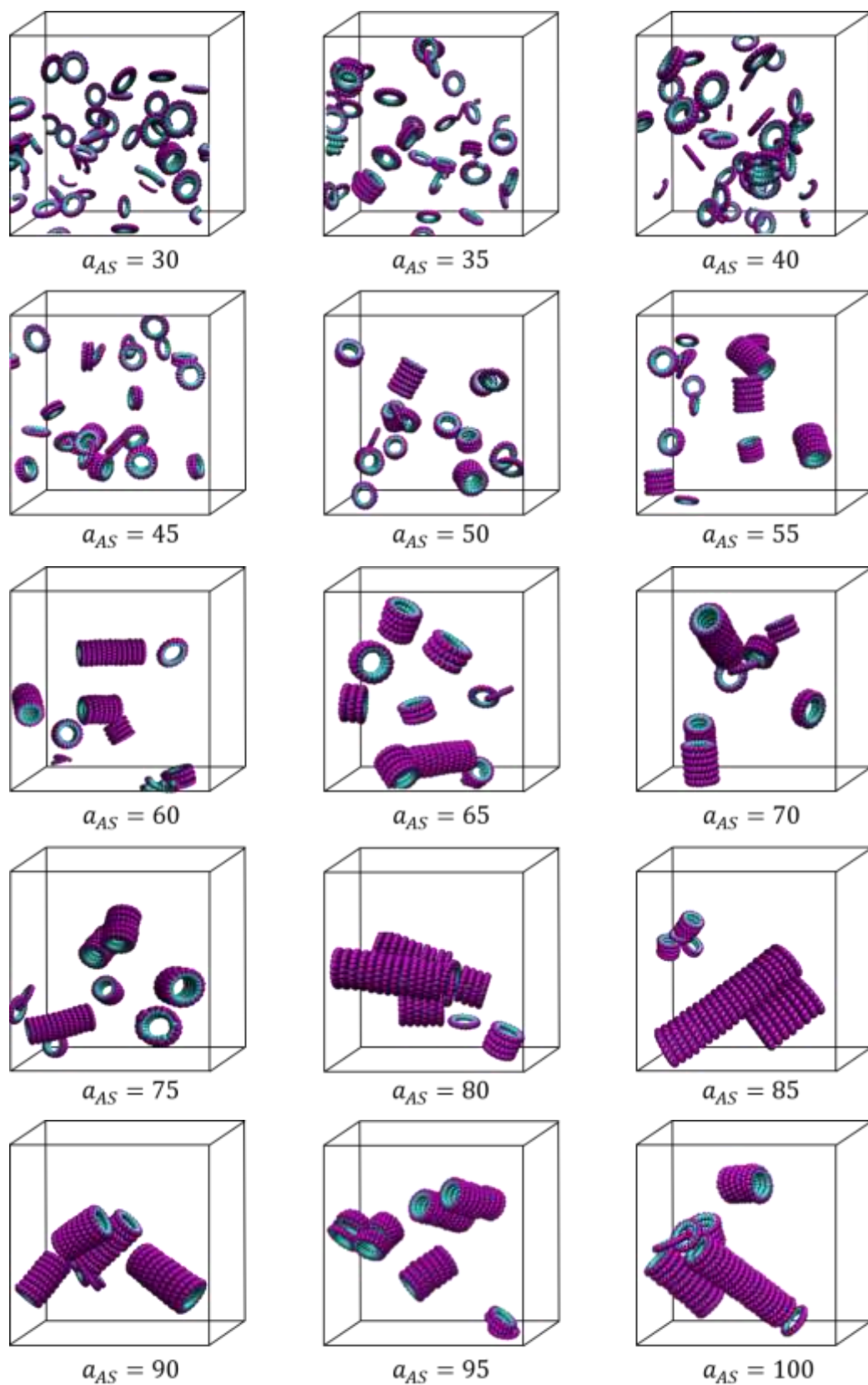


Figure S15. The snapshots of last frames extracted from MD trajectories in different values of a_{AS} , in which $\varphi=40$, $N=20$, $a_{BS}=25$ and $a_{AB}=90$.

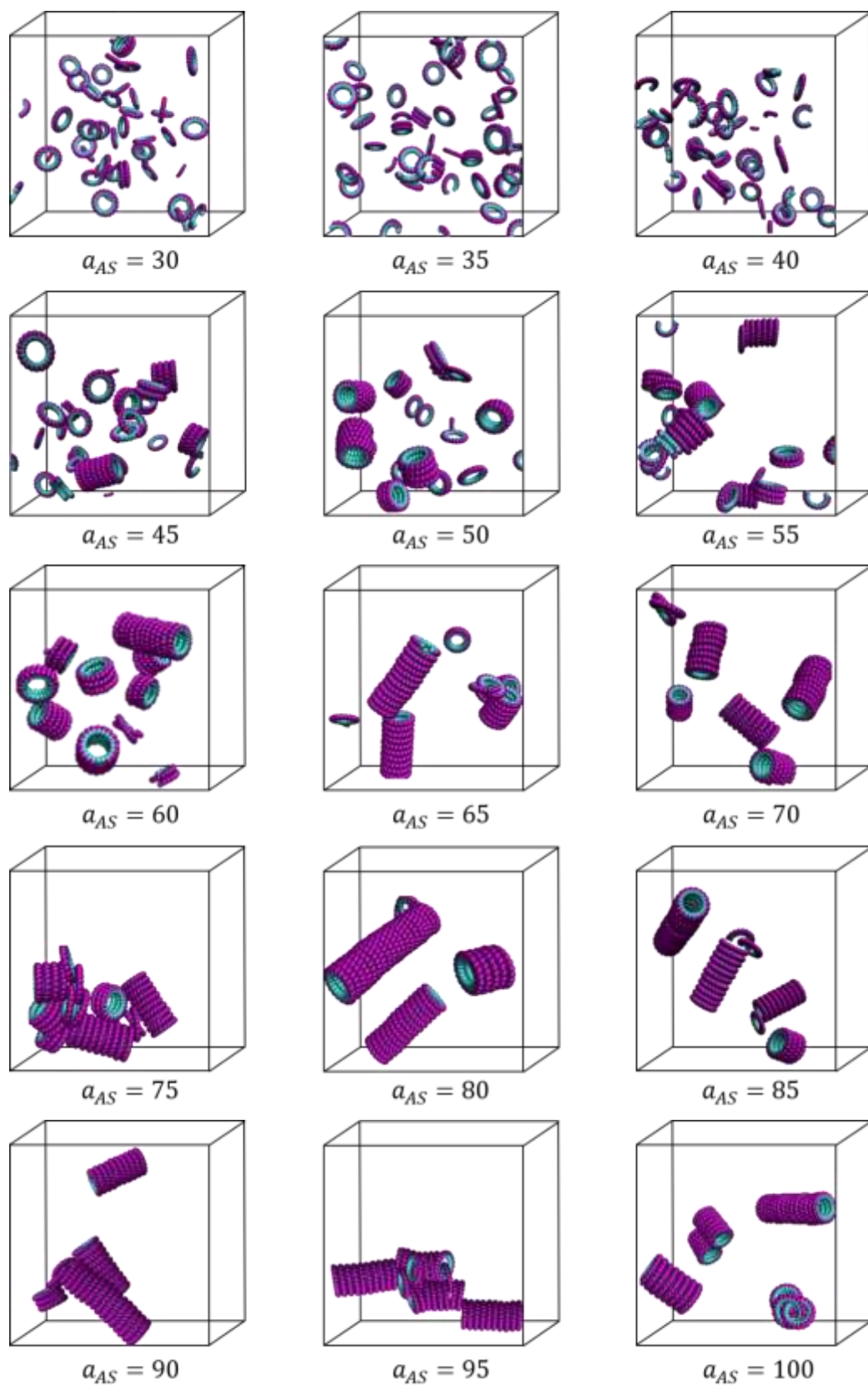


Figure S16. The snapshots of last frames extracted from MD trajectories in different values of a_{AS} , in which $\varphi=40$, $N=20$, $a_{BS}=25$ and $a_{AB}=95$.

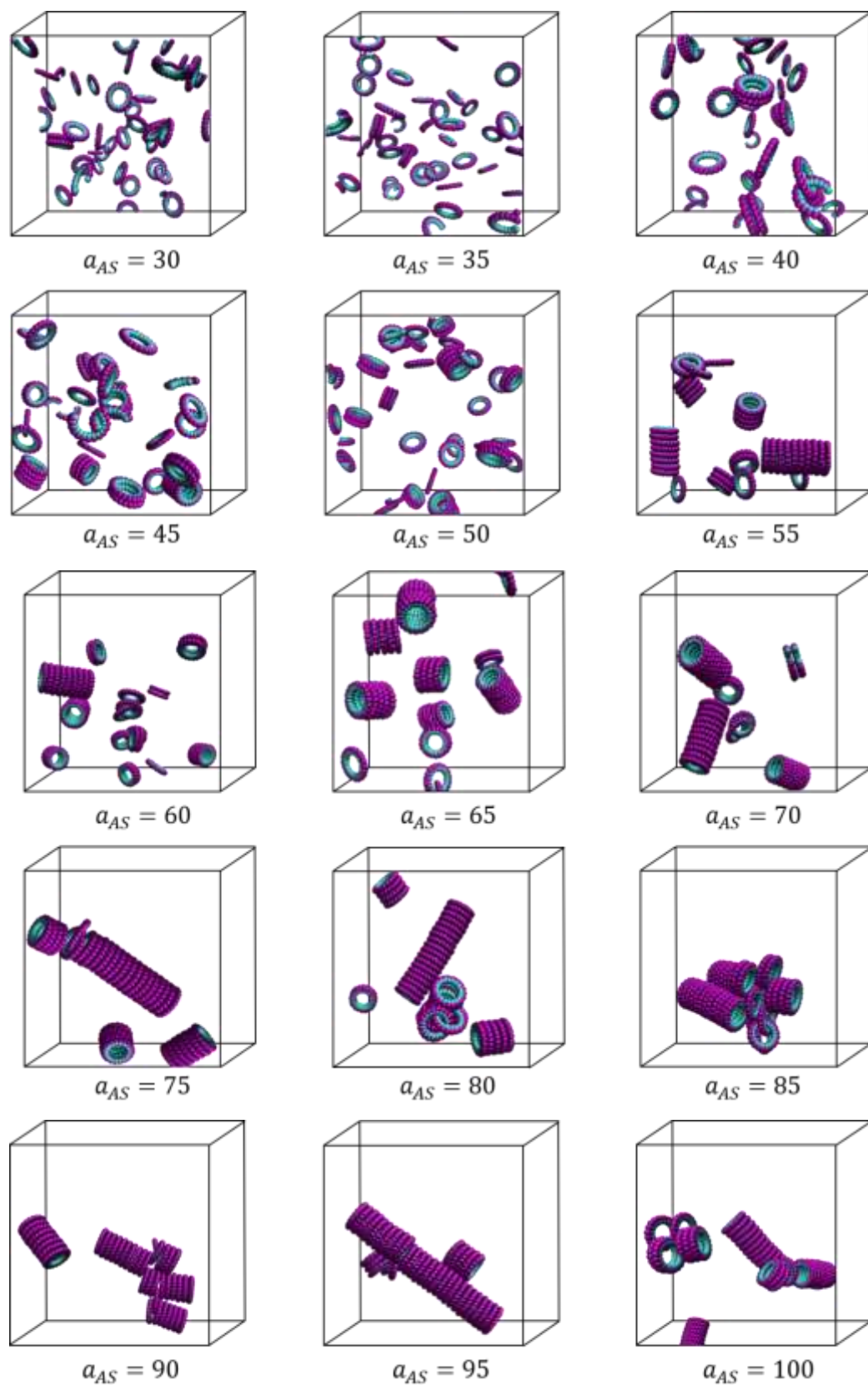


Figure S17. The snapshots of last frames extracted from MD trajectories in different values of a_{AS} , in which $\varphi=40$, $N=20$, $a_{BS}=25$ and $a_{AB}=100$.

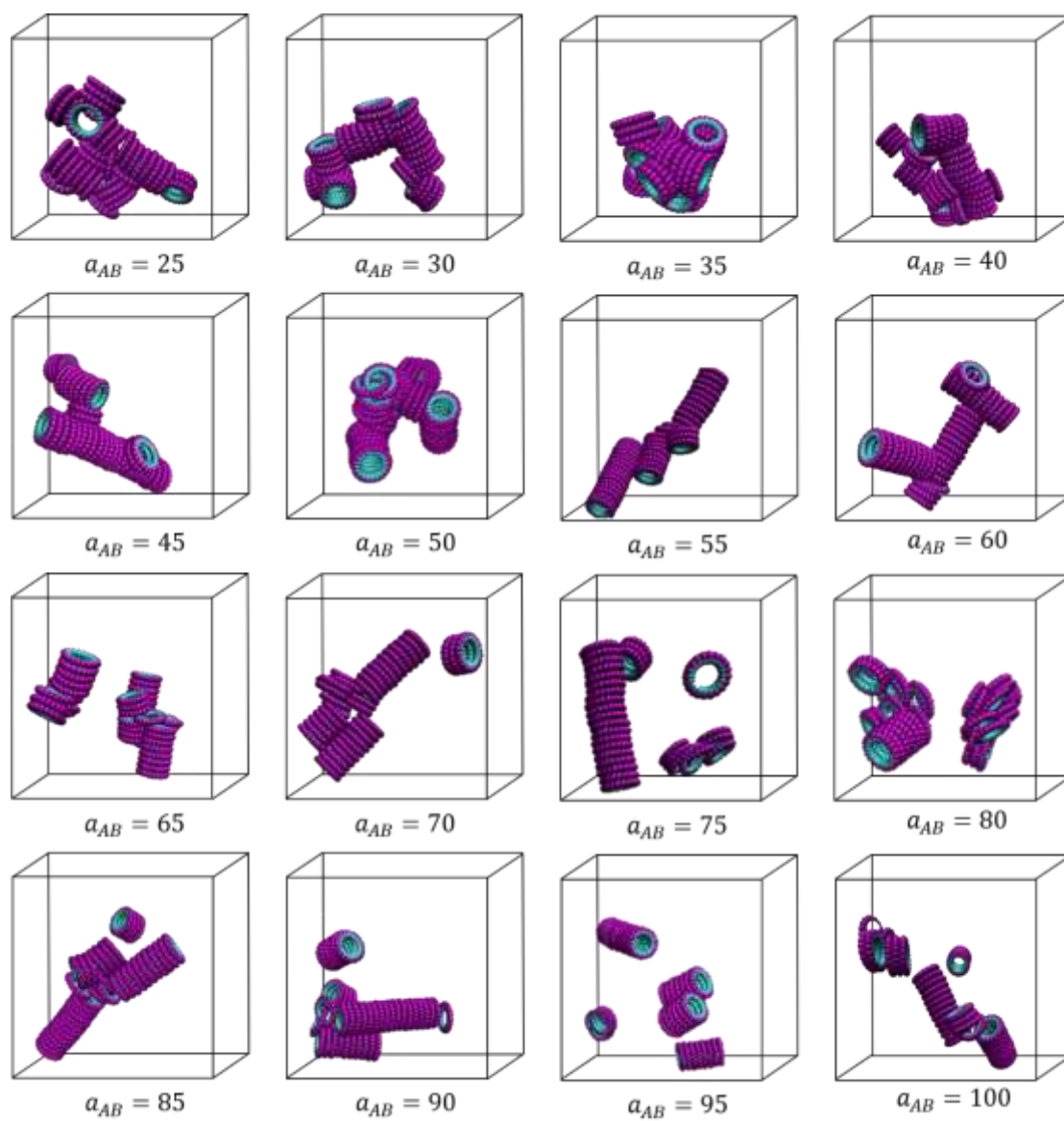


Figure S18. The snapshots of last frames extracted from MD trajectories in different values of α_{AB} , in which $\varphi=40$, $N=20$, $\alpha_{AS}=100$ and $\alpha_{BS}=25$.

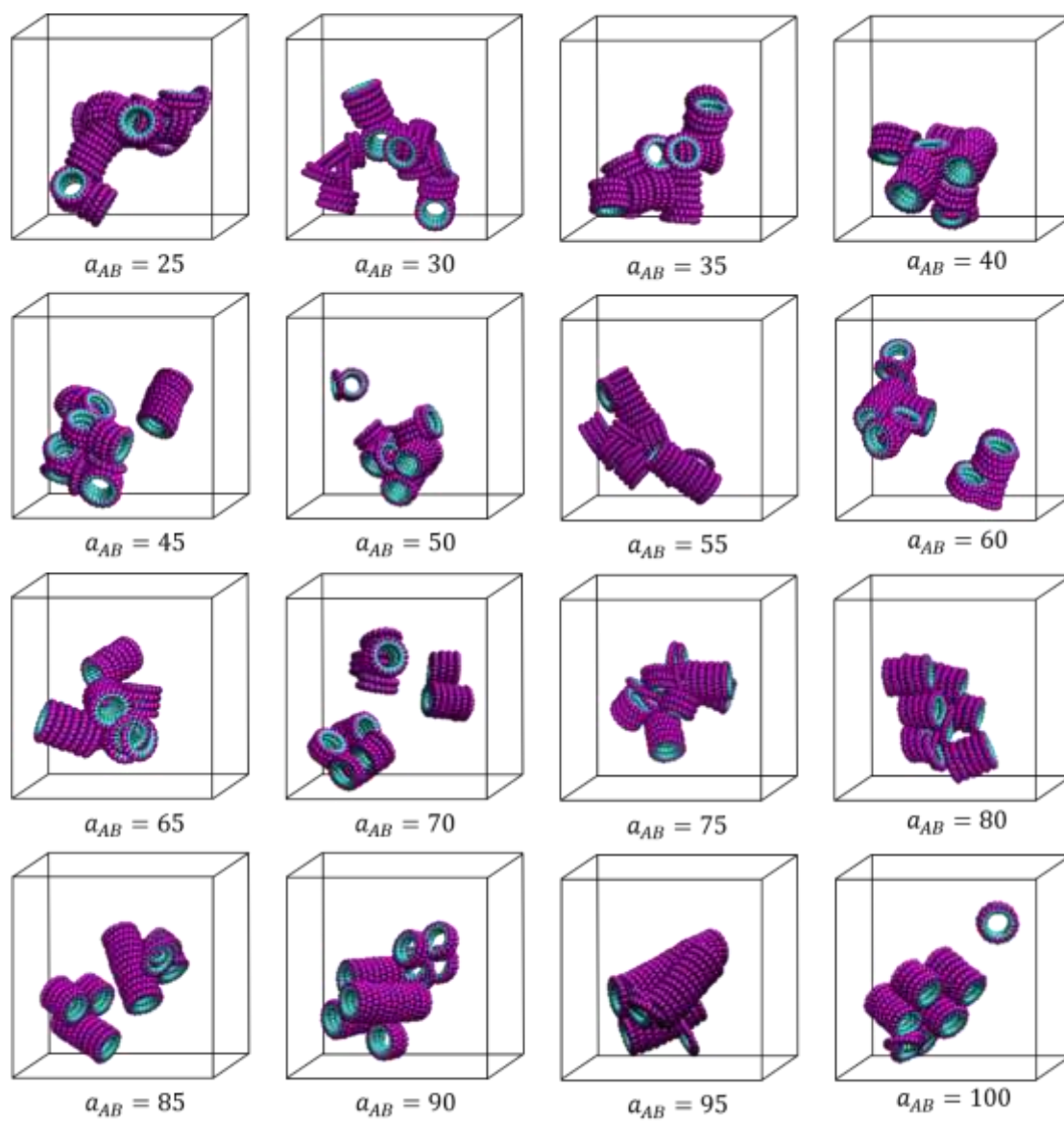


Figure S19. The snapshots of last frames extracted from MD trajectories in different values of α_{AB} , in which $\varphi=40$, $N=20$, $\alpha_{AS}=100$ and $\alpha_{BS}=30$.

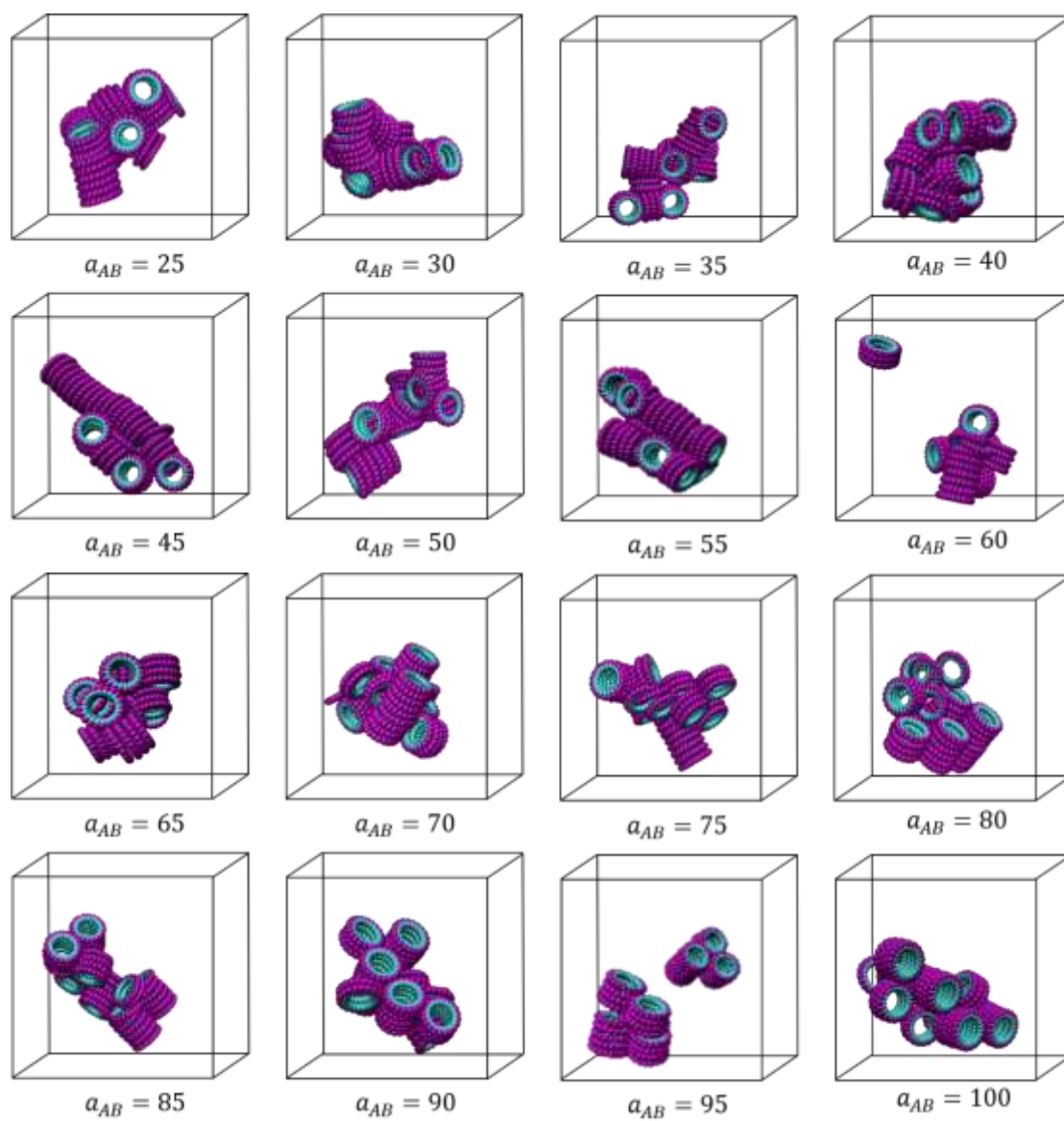


Figure S20. The snapshots of last frames extracted from MD trajectories in different values of α_{AB} , in which $\varphi=40$, $N=20$, $\alpha_{AS}=100$ and $\alpha_{BS}=35$.

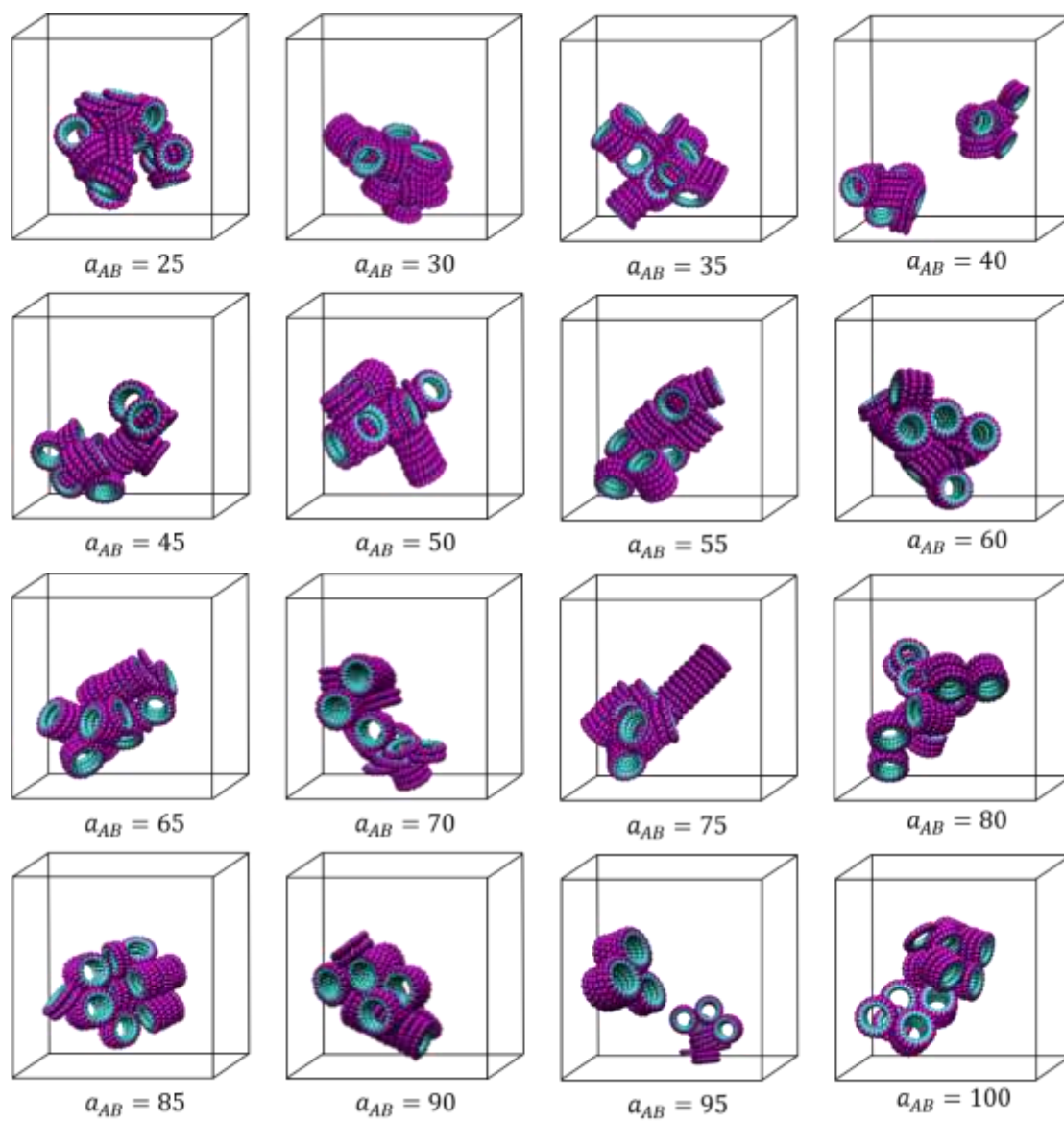


Figure S21. The snapshots of last frames extracted from MD trajectories in different values of α_{AB} , in which $\varphi=40$, $N=20$, $\alpha_{AS}=100$ and $\alpha_{BS}=40$.

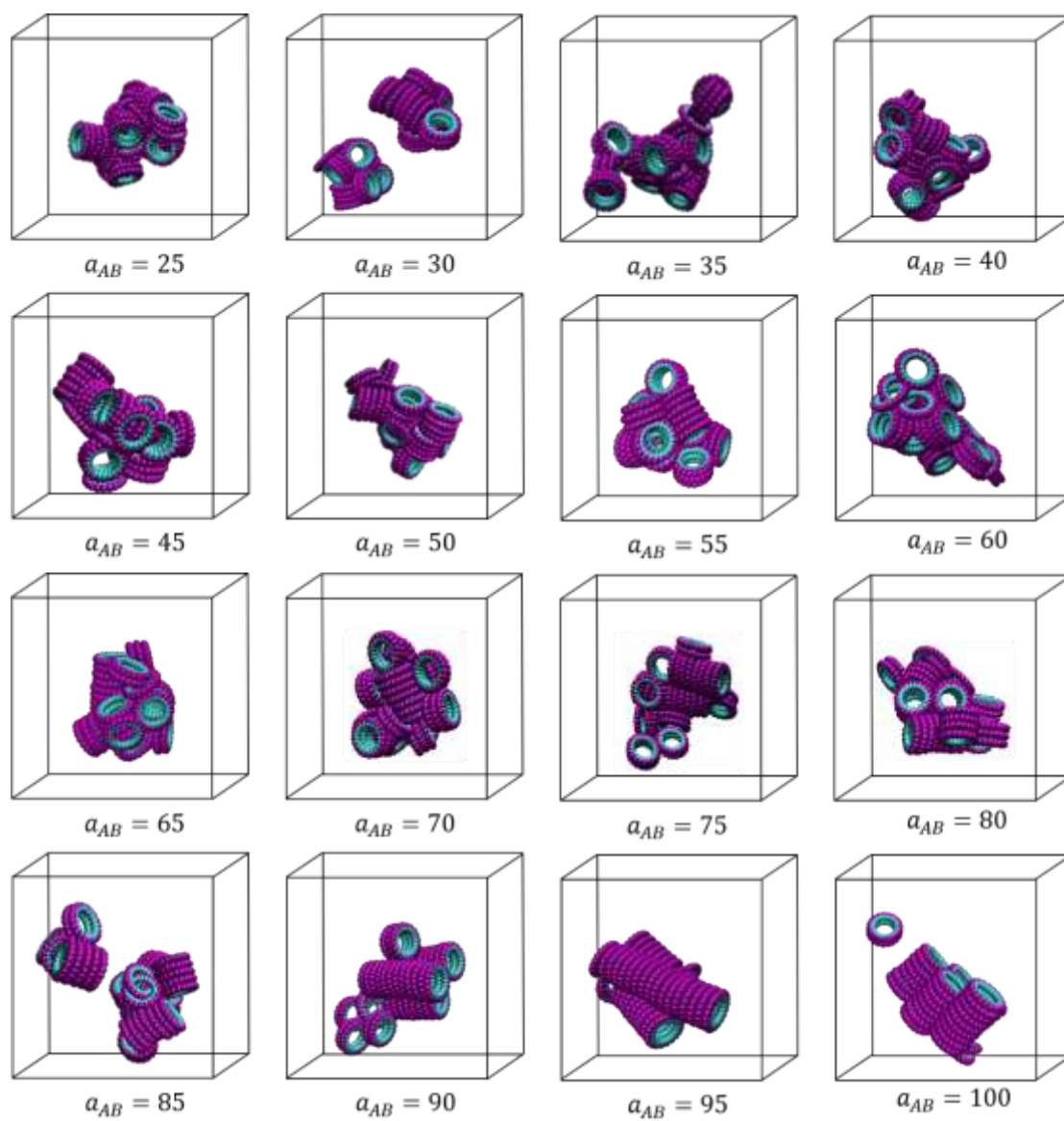


Figure S22. The snapshots of last frames extracted from MD trajectories in different values of α_{AB} , in which $\varphi=40$, $N=20$, $\alpha_{AS}=100$ and $\alpha_{BS}=45$.

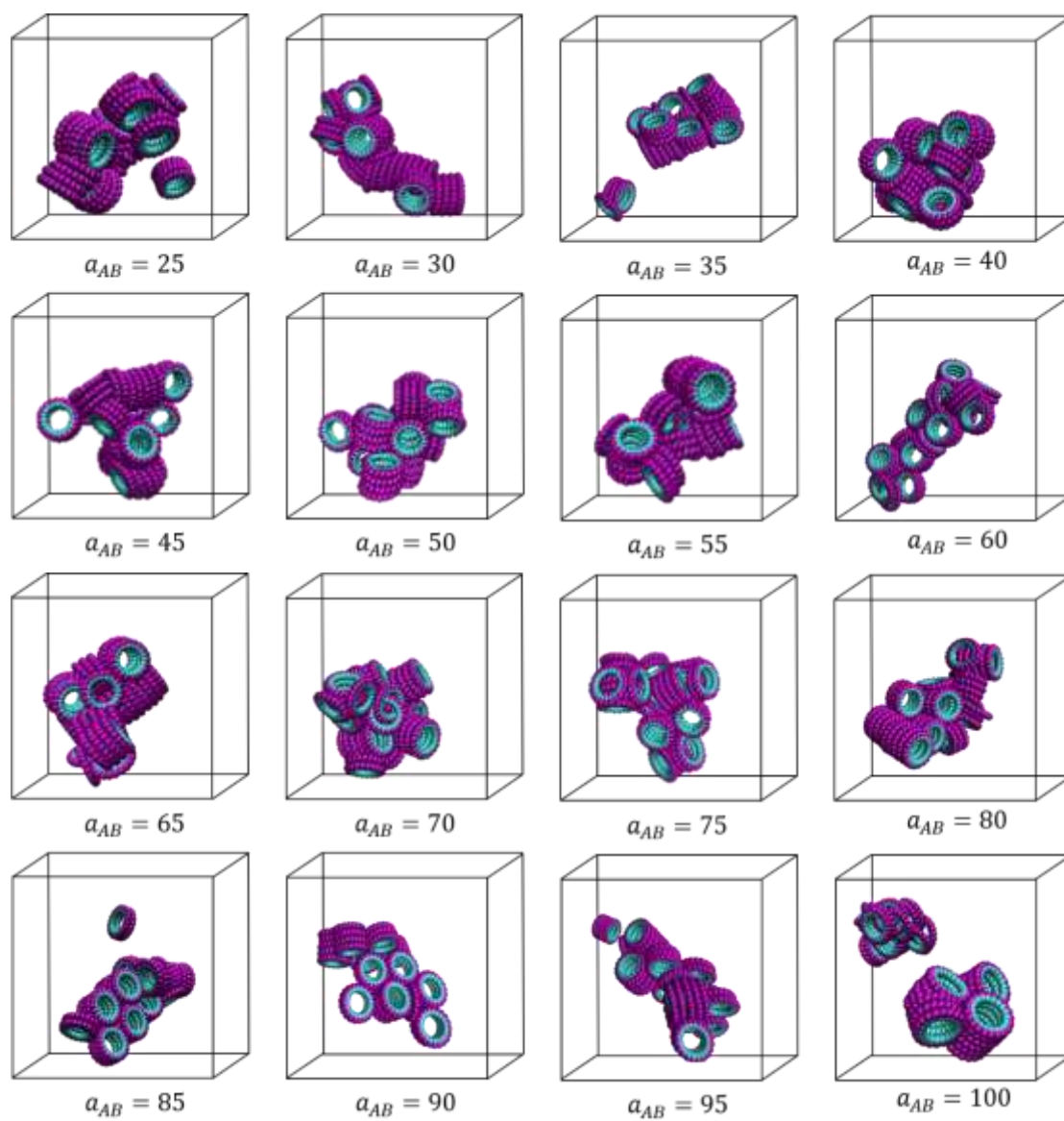


Figure S23. The snapshots of last frames extracted from MD trajectories in different values of α_{AB} , in which $\varphi=40$, $N=20$, $\alpha_{AS}=100$ and $\alpha_{BS}=50$.

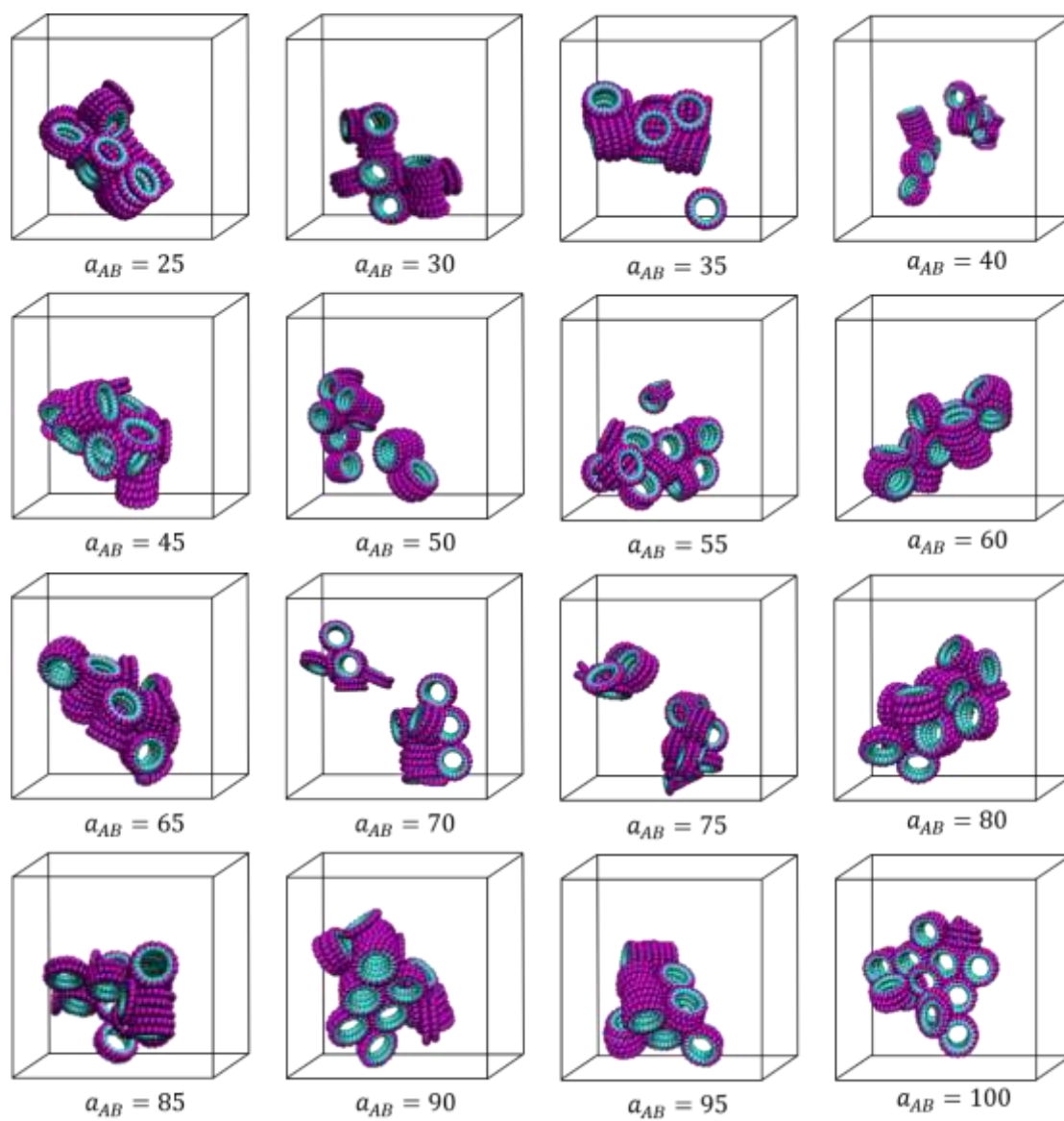


Figure S24. The snapshots of last frames extracted from MD trajectories in different values of a_{AB} , in which $\varphi=40$, $N=20$, $a_{AS}=100$ and $a_{BS}=55$.

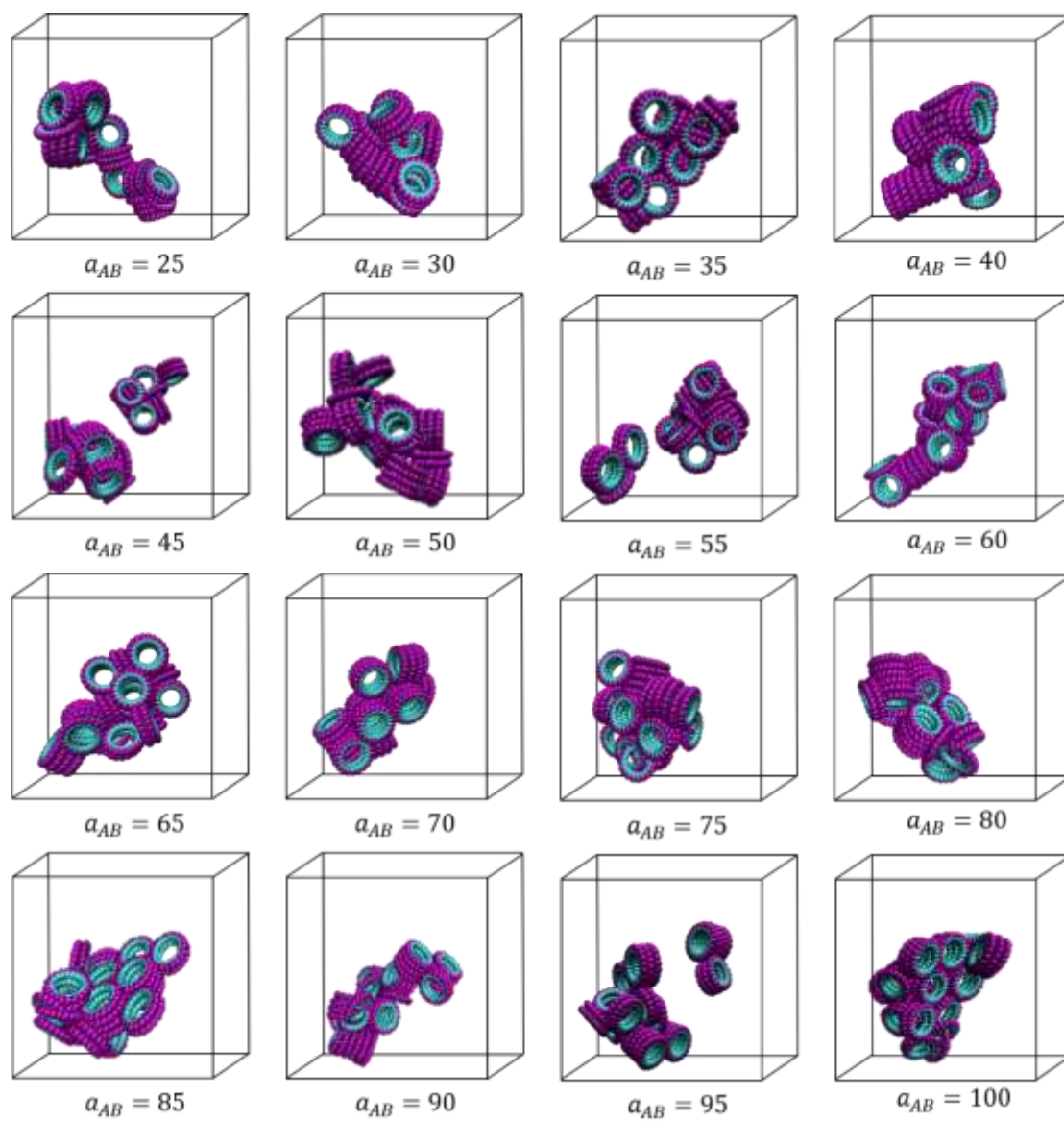


Figure S25. The snapshots of last frames extracted from MD trajectories in different values of α_{AB} , in which $\varphi=40$, $N=20$, $\alpha_{AS}=100$ and $\alpha_{BS}=60$.

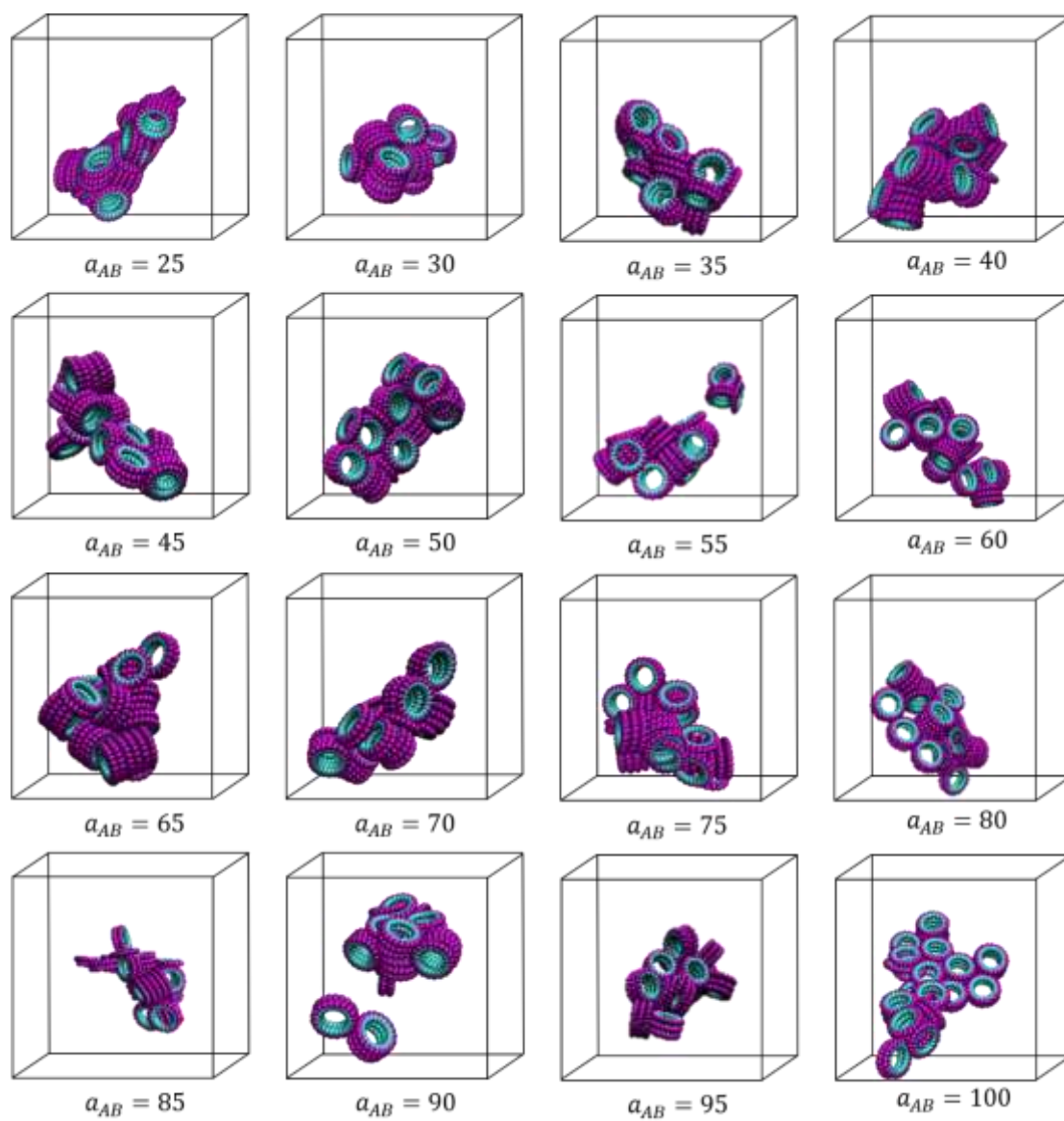


Figure S26. The snapshots of last frames extracted from MD trajectories in different values of α_{AB} , in which $\varphi=40$, $N=20$, $\alpha_{AS}=100$ and $\alpha_{BS}=65$.

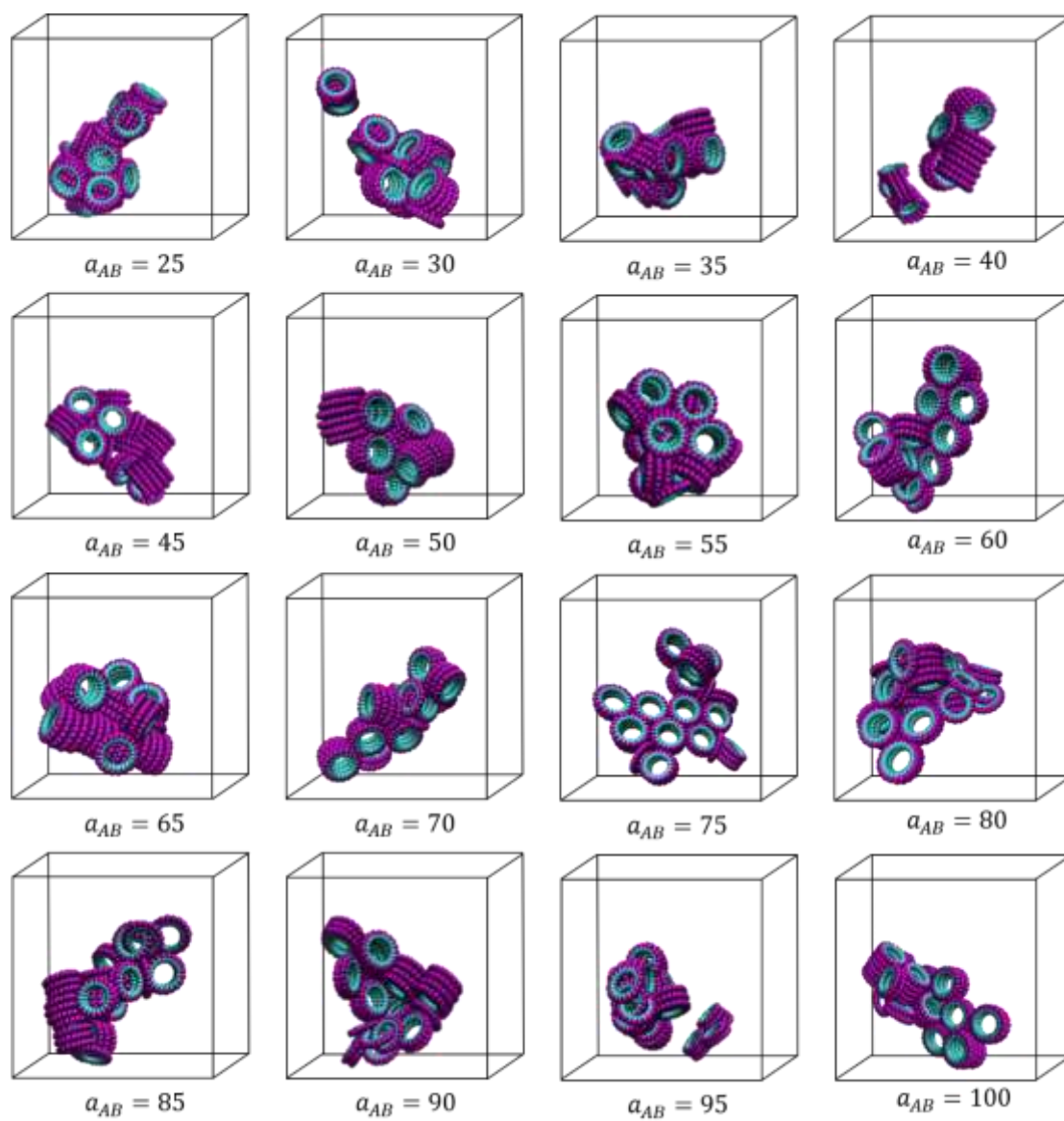


Figure S27. The snapshots of last frames extracted from MD trajectories in different values of α_{AB} , in which $\varphi=40$, $N=20$, $\alpha_{AS}=100$ and $\alpha_{BS}=70$.

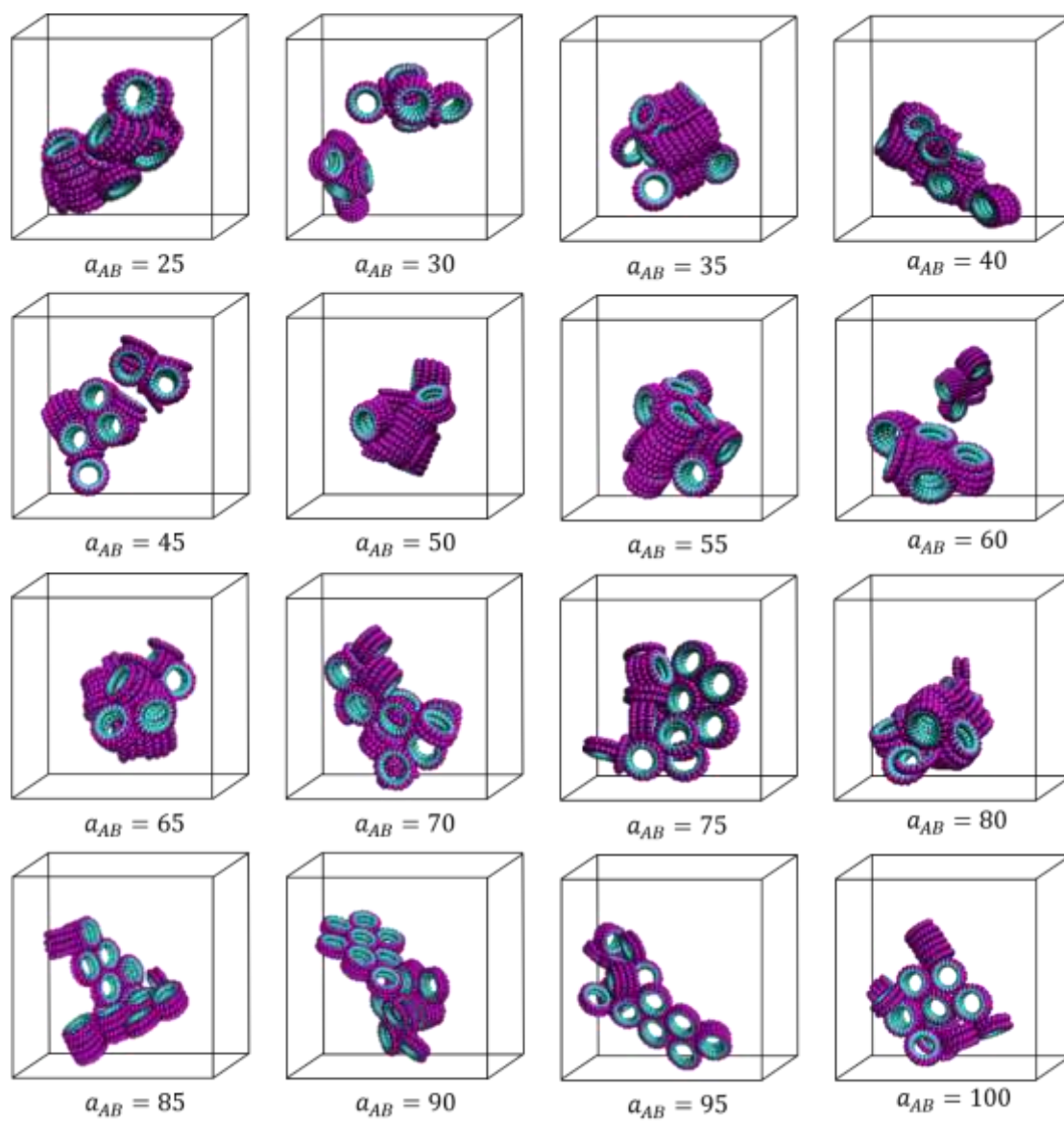


Figure S28. The snapshots of last frames extracted from MD trajectories in different values of α_{AB} , in which $\varphi=40$, $N=20$, $\alpha_{AS}=100$ and $\alpha_{BS}=75$.

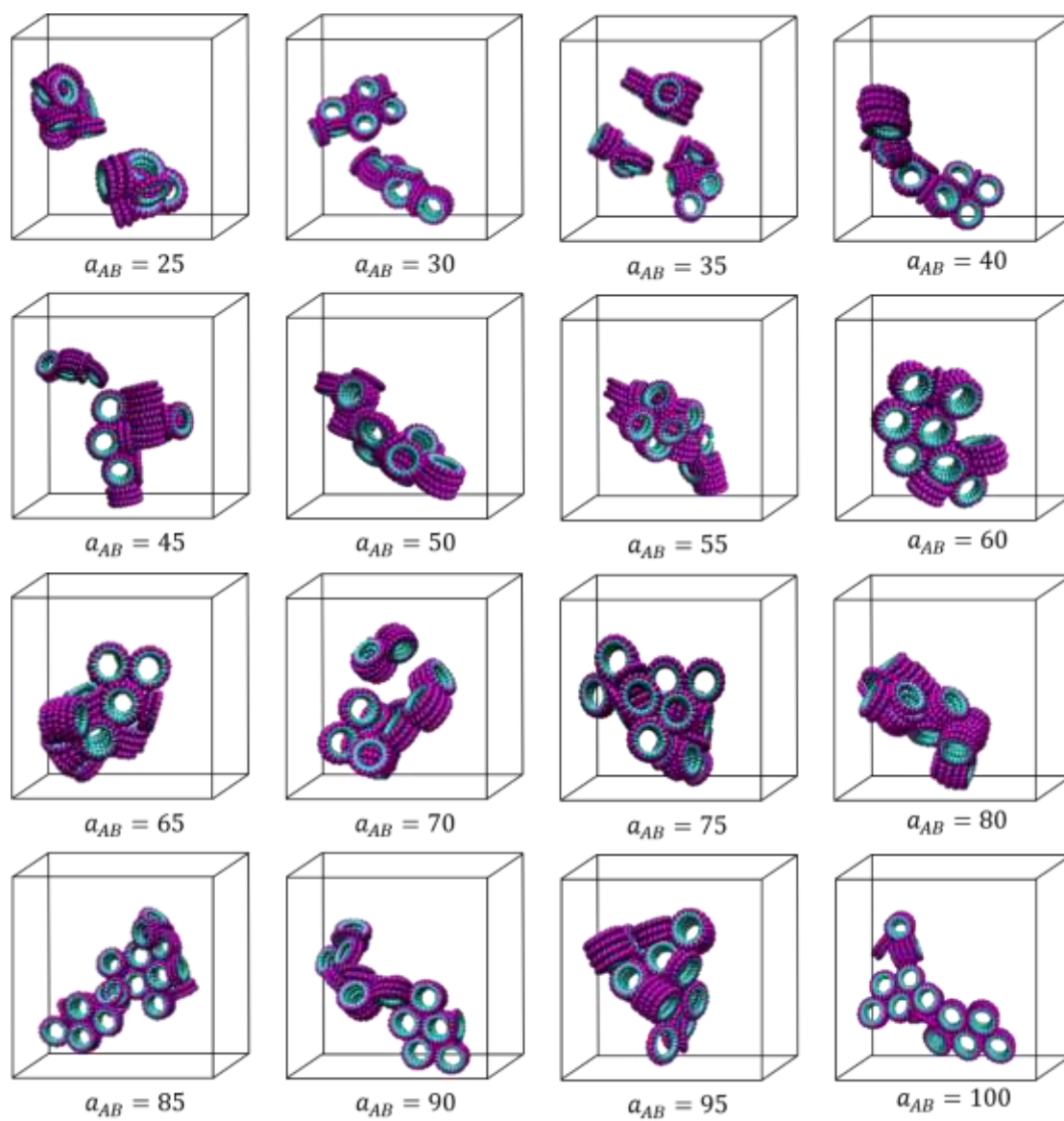


Figure S29. The snapshots of last frames extracted from MD trajectories in different values of a_{AB} , in which $\varphi=40$, $N=20$, $a_{AS}=100$ and $a_{BS}=80$.

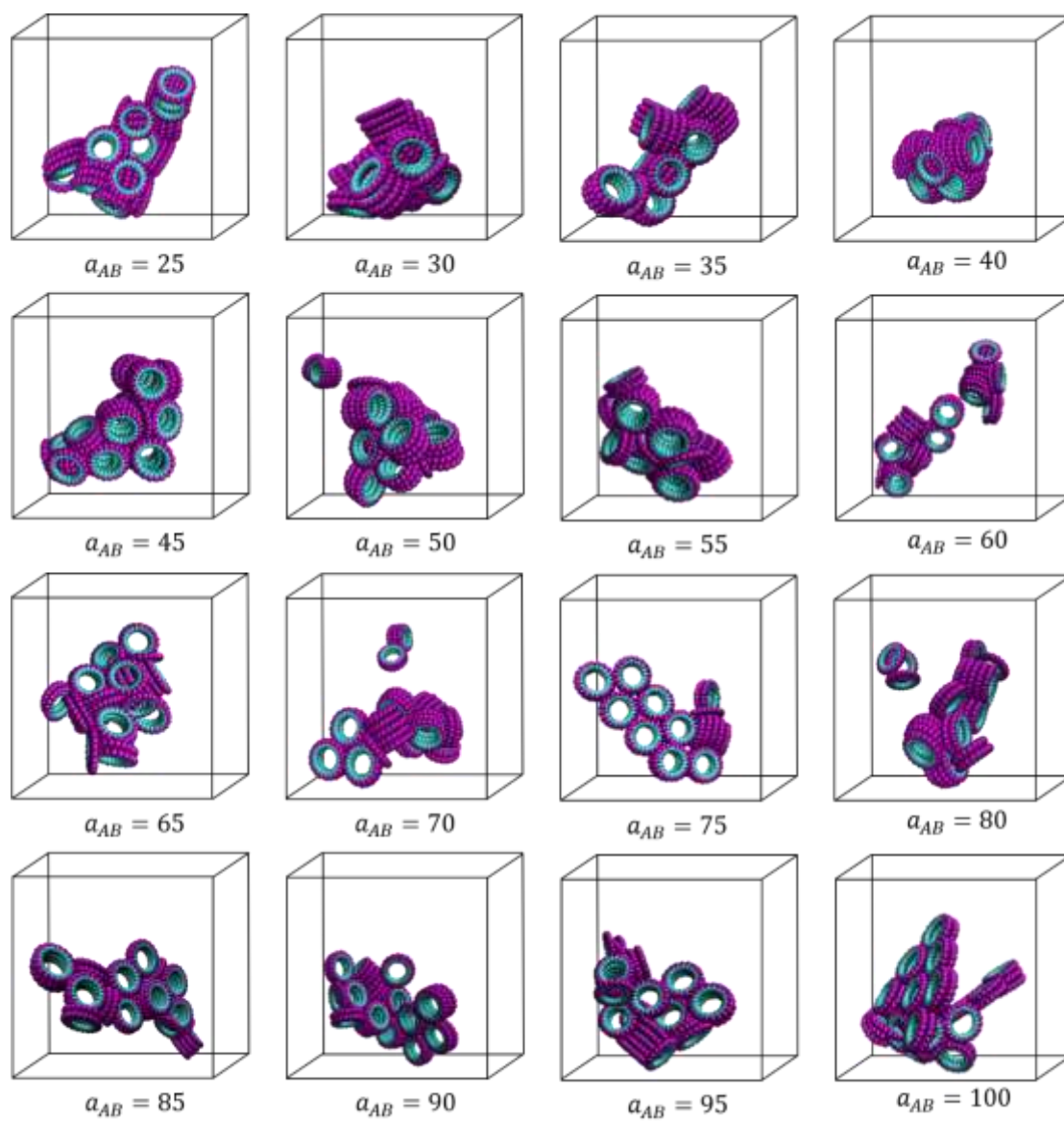


Figure S30. The snapshots of last frames extracted from MD trajectories in different values of α_{AB} , in which $\varphi=40$, $N=20$, $\alpha_{AS}=100$ and $\alpha_{BS}=85$.

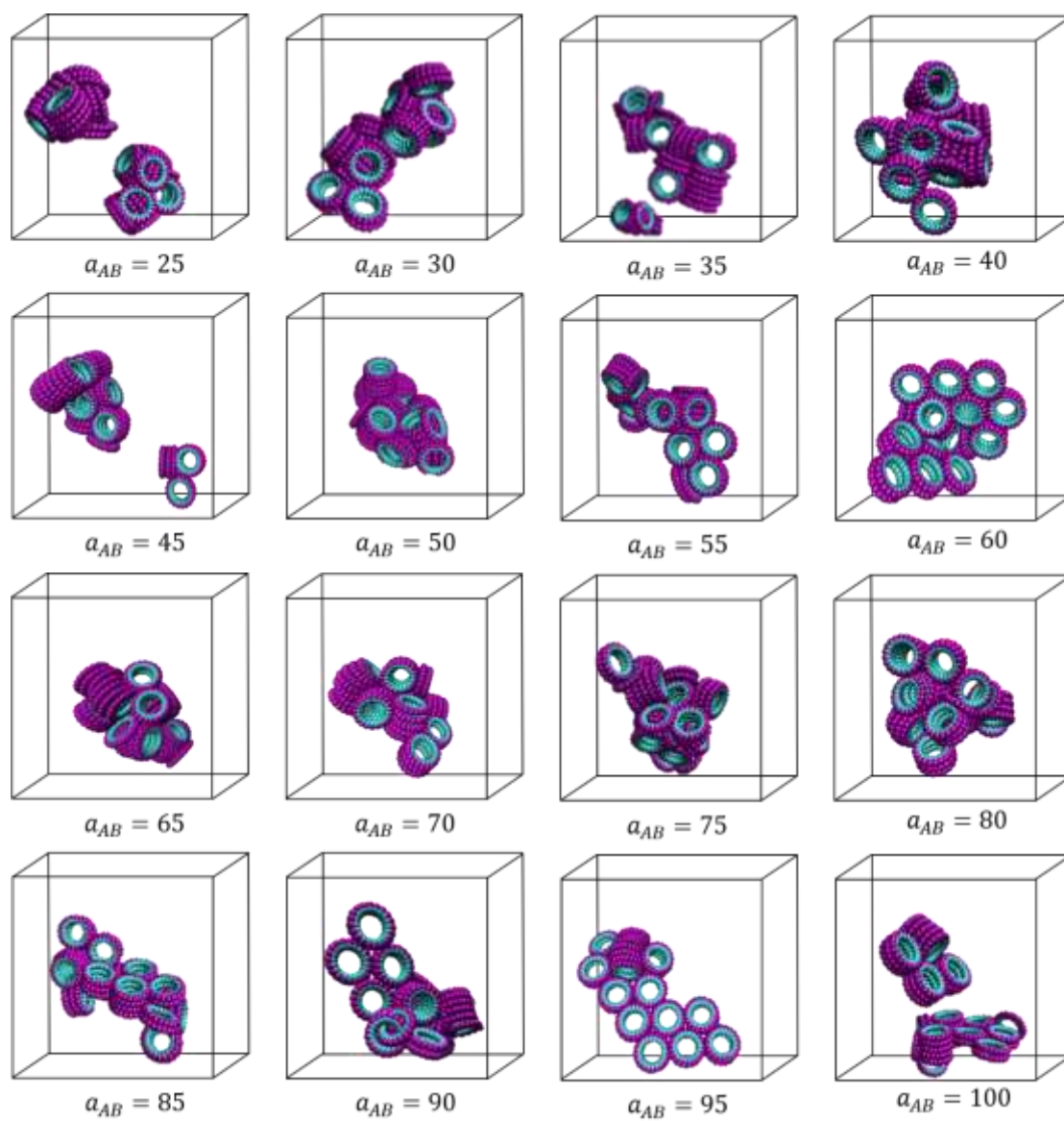


Figure S31. The snapshots of last frames extracted from MD trajectories in different values of a_{AB} , in which $\varphi=40$, $N=20$, $a_{AS}=100$ and $a_{BS}=90$.

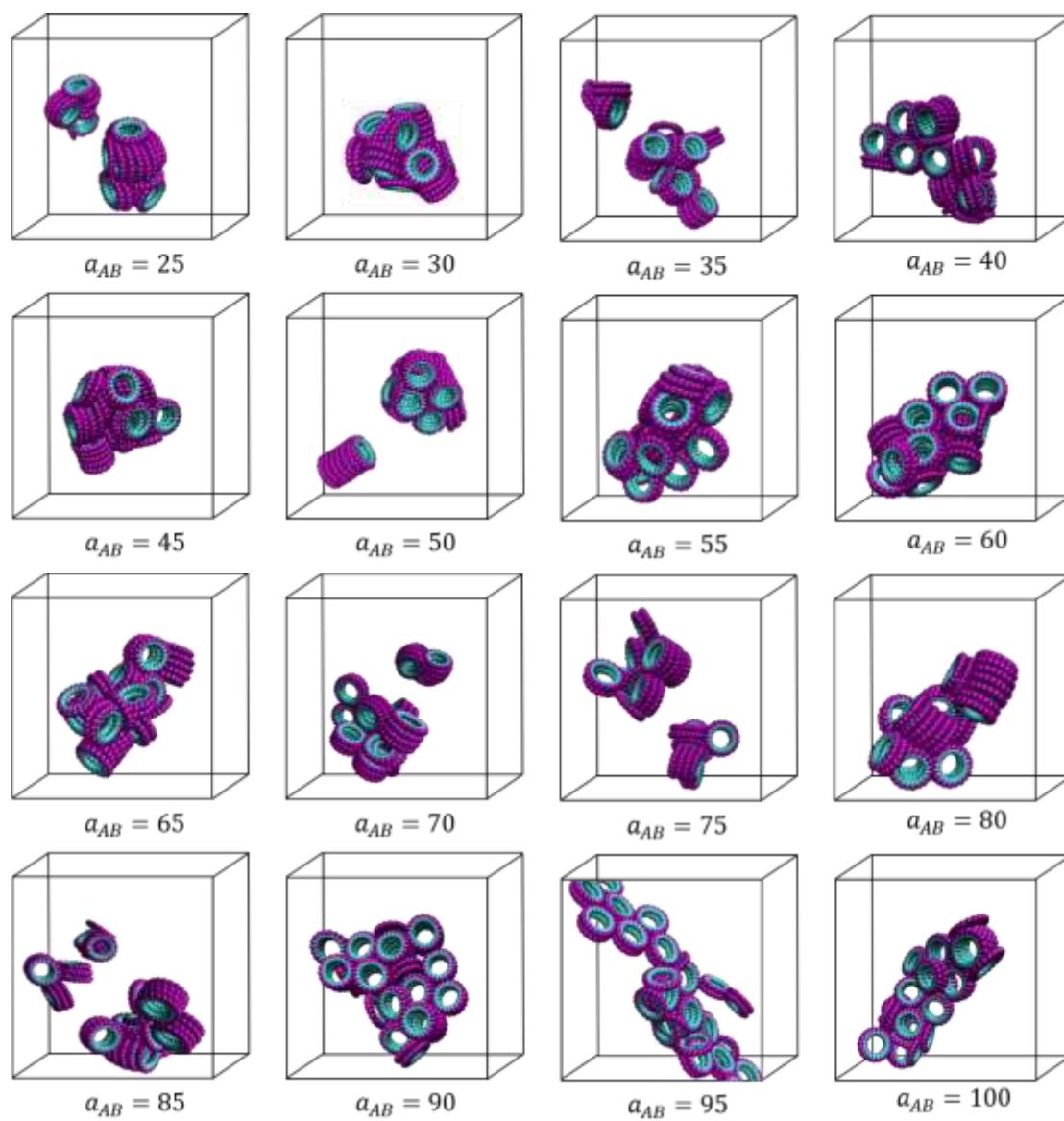


Figure S32. The snapshots of last frames extracted from MD trajectories in different values of α_{AB} , in which $\varphi=40$, $N=20$, $\alpha_{AS}=100$ and $\alpha_{BS}=95$.

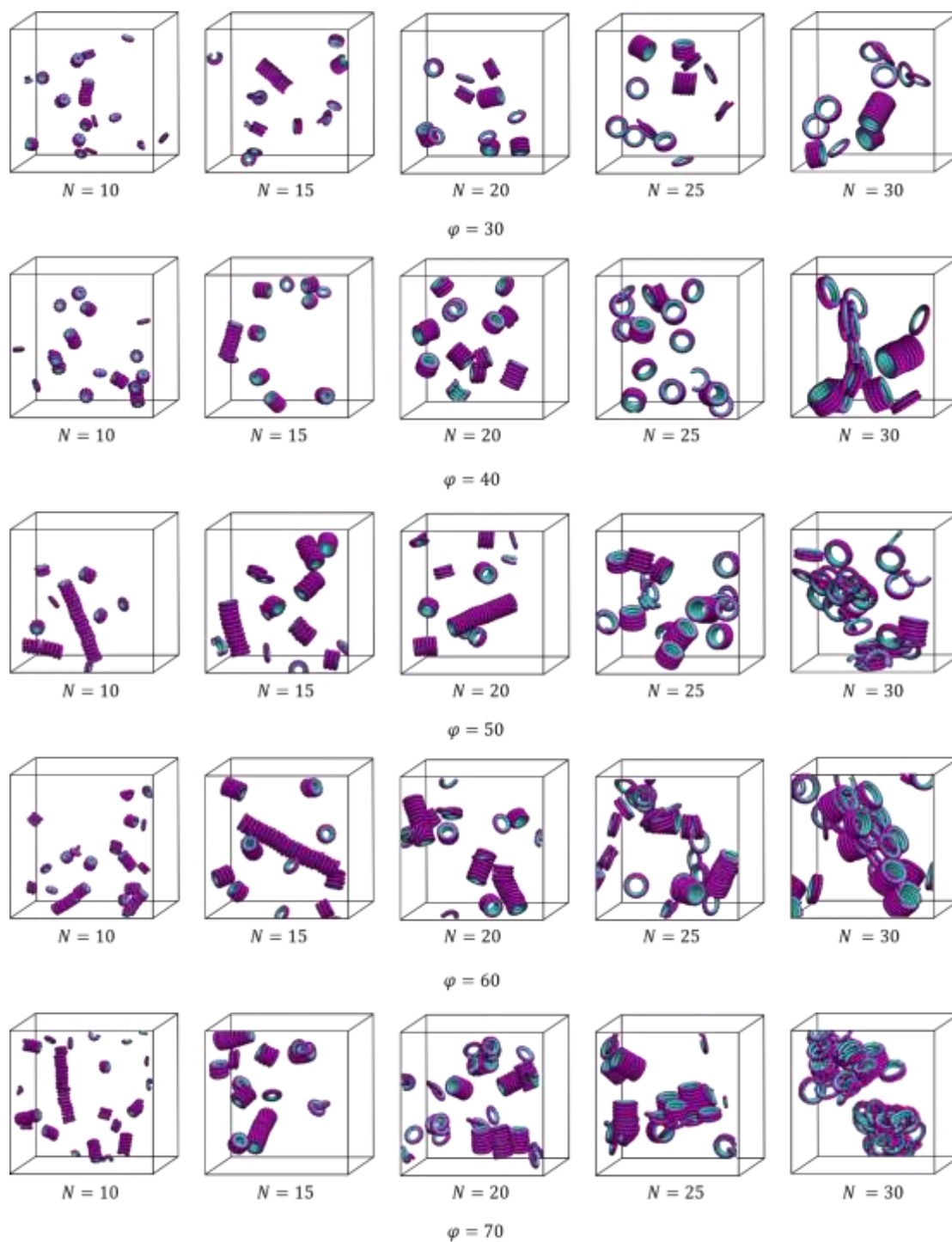


Figure S33. The snapshots of last frames extracted from MD trajectories in different values of N and φ , in which $a_{AS}=55$, $a_{BS}=100$ and $a_{AB}=55$.

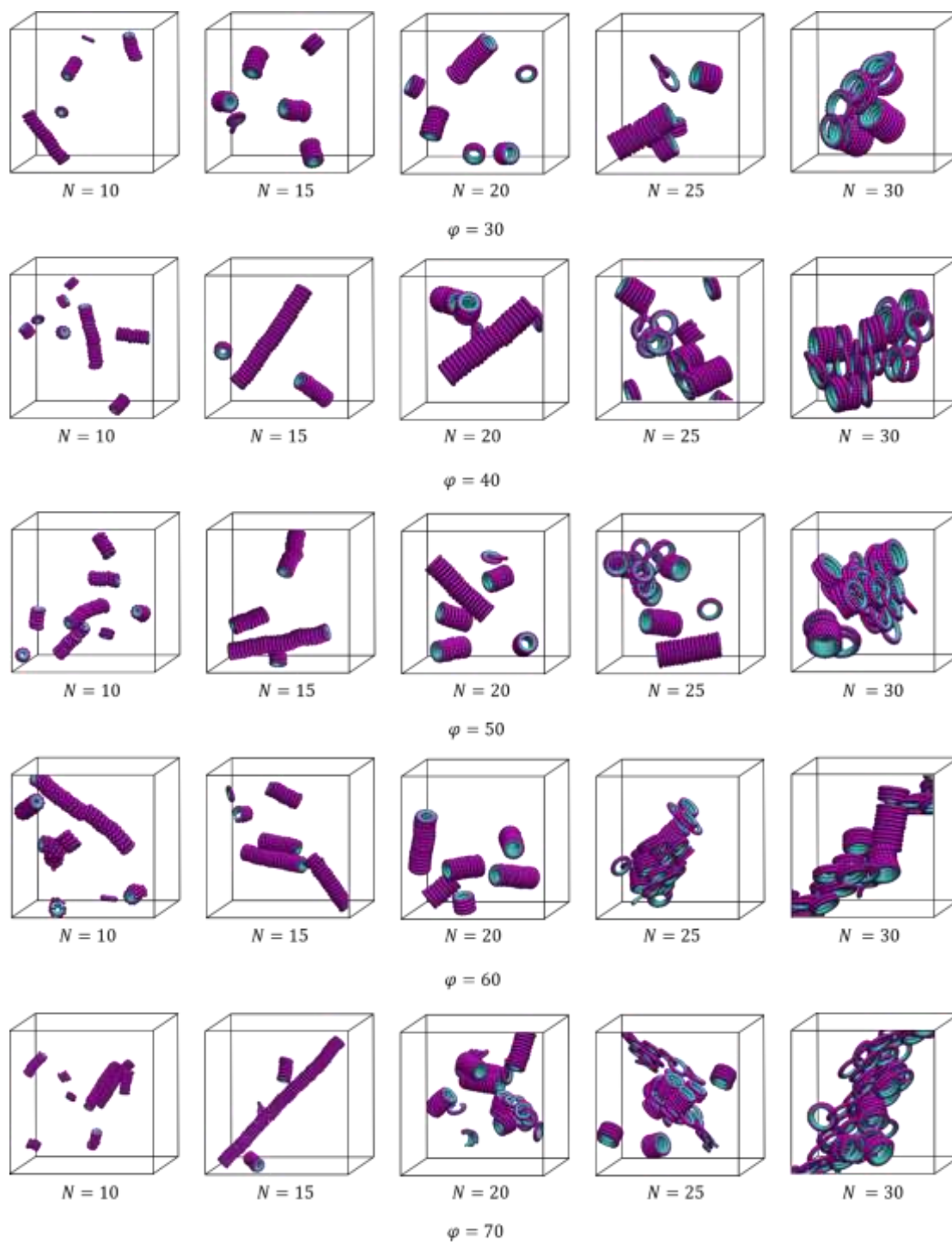


Figure S34. The snapshots of last frames extracted from MD trajectories in different values of N and φ , in which $a_{AS}=60$, $a_{BS}=100$ and $a_{AB}=65$.

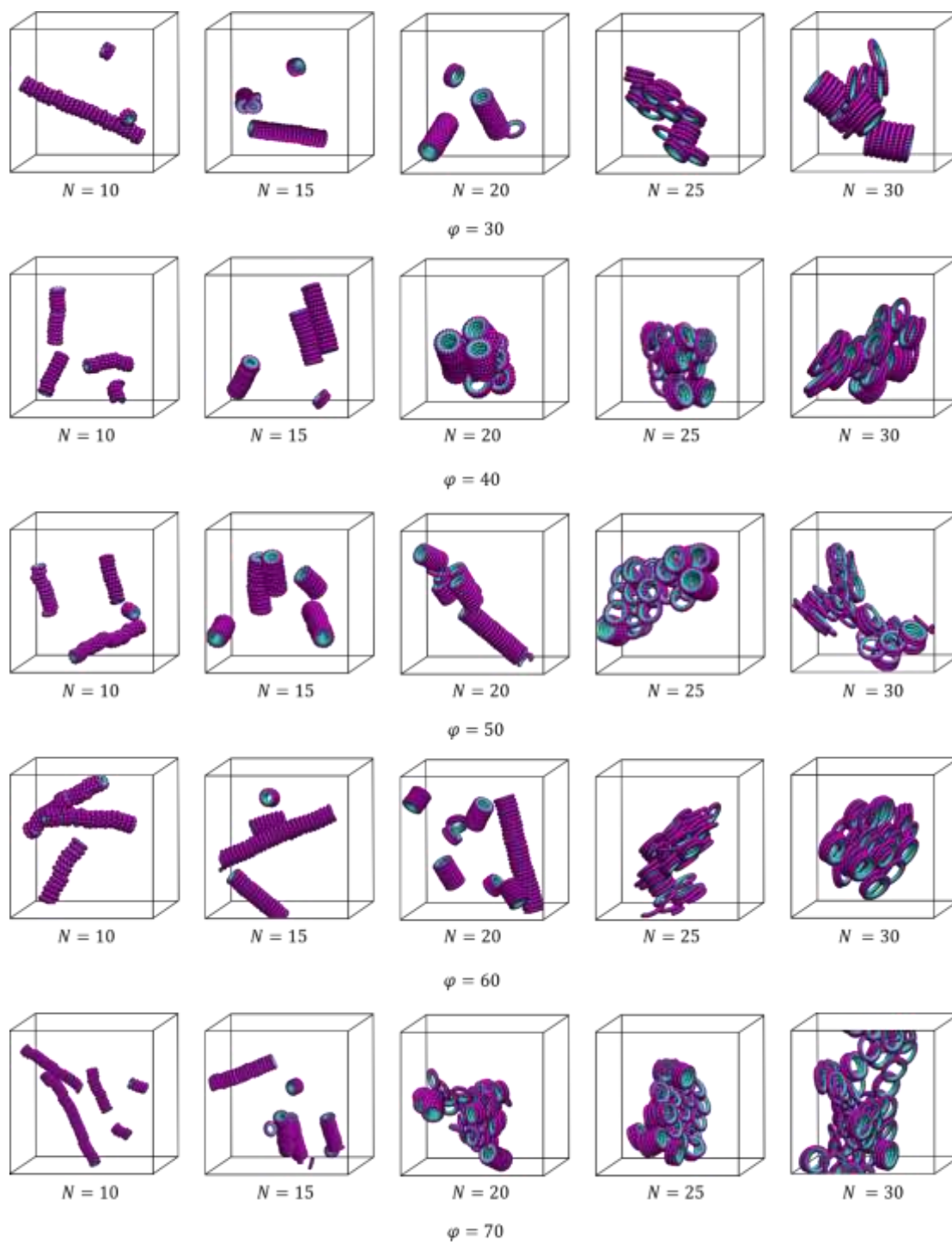


Figure S35. The snapshots of last frames extracted from MD trajectories in different values of N and φ , in which $a_{AS}=85$, $a_{BS}=100$ and $a_{AB}=100$.

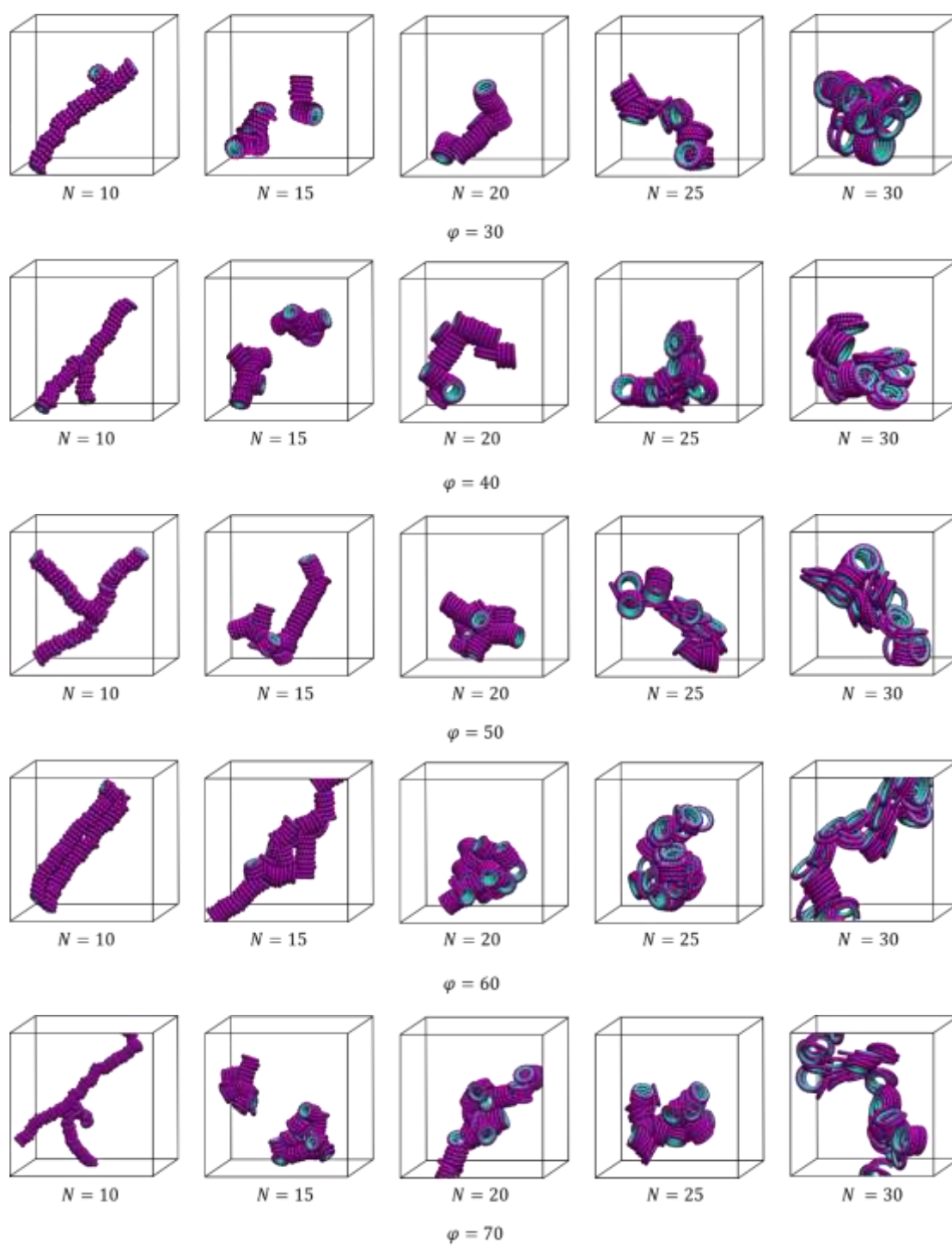
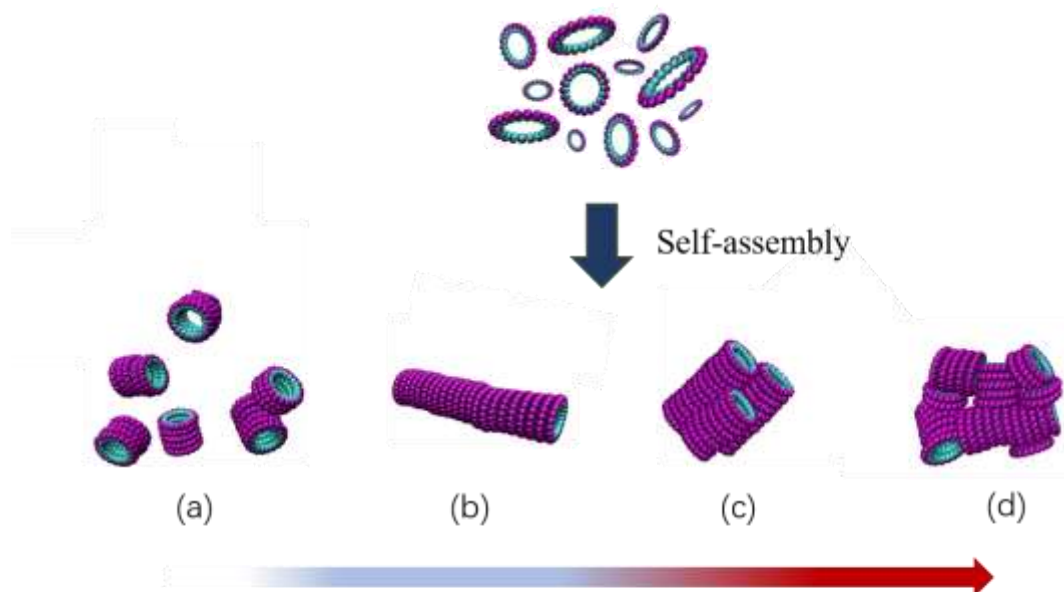


Figure S36. The snapshots of last frames extracted from MD trajectories in different values of N and φ , in which $a_{AS}=100$, $a_{BS}=100$ and $a_{AB}=30$.



The affinity of A and S decreases, and the affinity of A and B increases.

(A: hydrophobic bead; B: hydrophilic bead; S: solvent bead)

Figure S37. Summary of the phase transformation along the changes of simulation parameters, in which the interaction affinity of A and S decreases and the interaction between A and B increases. Herein, the parameters of $\varphi=40$ and $N=20$. In particular, (a) short independent channel; (b) long independent channel; (c) parallel channel; and (d) disordered channel.

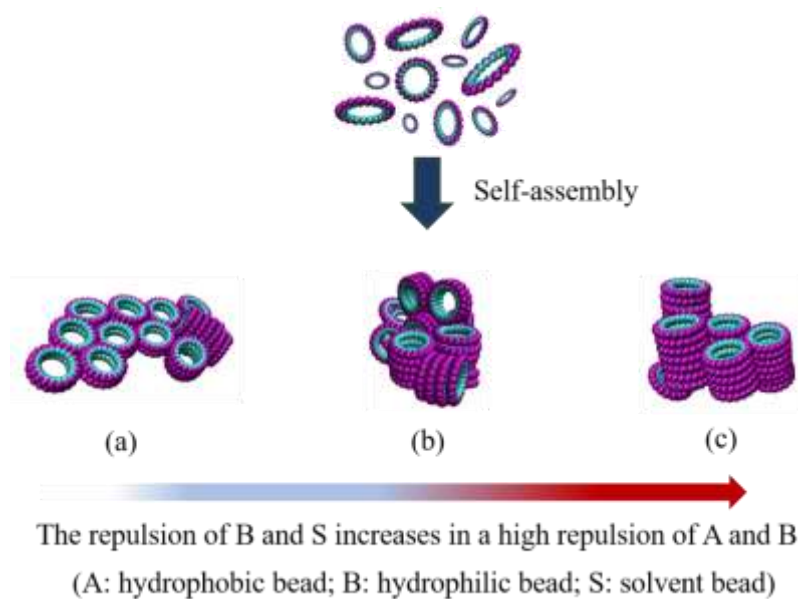


Figure S38. Summary of the phase transformation along the changes of simulation parameters, in which the repulsion of B and S beads increases. Herein, the parameters of $\varphi=40$ and $N=20$. Meanwhile, there is a big interaction parameter for A and B beads. In particular, (a) Laterally parallel channel; (b) disordered channel; and (c) vertically parallel channel.